AGS Proposal: Search for a permanent electric dipole moment of the deuteron nucleus at the 10^{-29} e · cm level.

D. Anastassopoulos,[21] V. Anastassopoulos,[21] D. Babusci,[8] M. Bai,[4] G. Bennett,[4] J. Bengtsson,[4] I. Ben-Zvi,[4] M. Blaskiewicz,[4] K. Brown,[4] G. Cantatore,[17] M. Dabaghyan,[20] V. Dzhordzhadze,[4] P.D. Eversheim,[2] M.E. Emirhan,[11] G. Fanourakis,[22] A. Facco,[13] A. Fedotov,[4] A. Ferrari,[8] T. Geralis,[22] Y. Giomataris,[23] F. Gonnella,[16] F. Gray,[18] R. Gupta,[4] S. Haciomeroglu,[11] G. Hoffstaetter,[6] H. Huang,[4] M. Incagli,[19] K. Jungmann,[9] M. Karuza,[17] D. Kawall,[14] B. Khazin,[5] I.B. Khriplovich,[5] I.A. Koop,[5] Y. Kuno,[15] D.M. Lazarus,[4] R. Larsen,[4] P. Levi Sandri,[8] F. Lin,[4] A. Luccio,[4] N. Malitsky,[4] W.W. MacKay,[4] W. Marciano,[4] A. Masaharu,[15] W. Meng,[4] R. Messi,[16] L. Miceli,[4] J.P. Miller,[3] D. Moricciani,[16] W.M. Morse,[4,a] C.J.G. Onderwater,[9,b] Y.F. Orlov,[6,c] C.S. Ozben,[11] T. Papaevangelou,[23] V. Ptitsyn,[4] B. Parker,[4] D. Raparia,[4] S. Redin,[5] S. Rescia,[4] G. Ruoso,[13] T. Russo,[4] A. Sato,[15] Y.K. Semertzidis,[4,*] Yu. Shatunov,[5] V. Shemelin,[6] A. Sidorin,[12] A. Silenko,[1] M. da Silva e Silva,[9] N. Simos,[4] E.J. Stephenson,[10,d] G. Venanzoni,[8] A. Vradis,[21] G. Zavattini,[7] A. Zelenski,[4] K. Zioutas[21]

[1]Research Inst. for Nucl. Probl. of Belarusian State University, Minsk, Belarus; [2]University of Bonn, Bonn, D-53115, Germany; [3]Boston University, Boston, MA 02215; [4]Brookhaven National Laboratory, Upton, NY 11973; [5]Budker Institute of Nuclear Physics, Novosibirsk, Russia; [6]Cornell University, Ithaca, NY 14853; [7]University and INFN, Ferrara, Italy; [8]Laboratori Nazionali di Frascati dell'INFN, Frascati, Italy; [9]University of Groningen, NL-9747AA Groningen, the Netherlands; [10]Indiana University Cyclotron Facility, Bloomington, IN 47408; [11]Istanbul Technical University, Istanbul 34469, Turkey; [12]Joint Institute for Nuclear Research, Dubna, Moscow region, Russia; [13]Legnaro National Laboratories of INFN, Legnaro, Italy; [14]University of Massachusetts, Amherst, MA 01003; [15]Osaka University, Osaka, Japan; [16]Dipartimento di Fisica, Universita' "Tor Vergata" and Sezione INFN, Rome, Italy; [17]University and INFN Trieste, Italy; [18]Physics Dept., Regis University, Denver, CO 80221; [19]University and INFN Pisa, Italy; [20]Brigham and Women's Hospital, Harvard Medical School, Boston, MA 02115; [21]University of Patras, Patras, Greece; [22]Institute of Nuclear Physics Dimokritos, Athens, Greece; [23]Saclay/Paris, France

April, 2008

Requesting 4×10^{11} vector polarized, bunched, 1 GeV/c total momentum deuterons per 10^3 s cycle. Total running time 5000 hours.

* Interim Spokesperson, semertzidis@bnl.gov, +1(631)344-3881

[a] Int. deputy Spokesperson for Systematic errors, morse@bnl.gov, +1(631)344-3859

[b] Int. deputy Spokesperson for DAQ & Electronics, onderwater@kvi.nl, +31(50)363-3557

[c] Int. deputy Spokesperson for beam & spin dynamics, yfo1@cornell.edu, +1(607)255-3502

[d] Int. deputy Spokesperson for polarimetry, stephene@indiana.edu, +1(812)855-5469.

Abstract

We propose using the storage ring method to measure the electric dipole moment (EDM) of D^+, the bare deuteron nucleus, with a one sigma sensitivity of $10^{-29}\,e\cdot cm$ per 10^7 s running time. At this level it will be the best experiment among current and currently planned EDM experiments. Its mass scale reach for SUSY-type new physics is more than 300 TeV, or if there is physics at the LHC scale, its sensitivity to CP-violating phases is 10^{-5} rad; both scales are much beyond the design sensitivity of the LHC.

High intensity, polarized deuteron sources, polarimeters with high analyzing powers at 1 GeV/c total deuteron momentum, and the application of common accelerator techniques make this goal possible. The polarimeter systematic errors are minimized by applying symmetries related to the deuteron spin direction and the EDM signal. In addition, the slow beam extraction onto a solid carbon target aided by a precise beam position monitoring system ensures that the beam direction axis will remain the same within very tight limits during the storage time. The widening of the polarimeter detector capabilities to give counting as well as directional information will severely restrict the larger polarimeter systematic errors to well below the 10^{-29} e·cm level. We are perfecting those techniques by running very important hardware tests at KVI (the Netherlands) and COSY (Germany), where polarized deuteron beams are currently available.

Contents

1 Introduction

In this proposal, we discuss a completely new approach to EDM studies employing a charged particle storage ring. An intense electric field appears in the particle rest frame due to the applied laboratory dipole-magnet B-field, which, acting on a EDM, affects the observed spin precession. This novel technique promises significant sensitivity improvements for the deuteron and perhaps other charged ion systems, and is complementary to the neutron and neutral atom experiments. So far, the deuteron (a stable spin 1, pn bound state) appears to be the best charged particle candidate capable of reaching a sensitivity of $10^{-29}\,\mathrm{e}\cdot\mathrm{cm}$. That phenomenal capability promises to provide a powerful probe of new physics and new CP-violation, with potential discovery rivaling or exceeding other methods such as those of ultra-cold neutrons or atoms.

The quest for physics beyond the Standard Model (SM) currently represents a major effort in basic physics research. Since the Electric Dipole Moment (EDM) values predicted by most extensions to the SM are many orders of magnitude larger than those of the SM itself and close to present sensitivity limits, EDM experiments have become very sensitive probes for new physics. Future searches will either locate an EDM or severely constrain SM extensions. Furthermore, a non-vanishing EDM is a violation of T and P symmetries, and under the assumption of CPT invariance would imply a new source of CP violation, perhaps shedding light on the puzzling baryon/anti-baryon asymmetry of the universe. Even if an EDM is found in another experiment, multiple observations will be needed to characterize the form of the CP violation. Indeed, EDM searches have already helped to shape our knowledge of fundamental particles and interactions for more than half a century. From the early, pioneering experiments on the neutron in the 1950s [1], limits on both neutron and atomic EDMs have been improved by many orders of magnitude. However, it is striking to note that so far, all sensitive searches have been performed on neutral systems. EDM limits on the charged constituents have been inferred with theoretical estimates. In our proposed experiment the EDM of D^+, the bare deuteron nucleus, is probed *directly* using a storage ring technique which has the potential to increase the sensitivity of EDM measurements by several orders of magnitude.

Our storage ring EDM collaboration has extensively studied three methods of probing EDMs in storage rings: The frozen spin method (FSM) [2], the resonance method [3], and the spin dressing method [4]. Based on its extensive experience working for several years on the FSM, the collaboration has confidence that the FSM surpasses all the others. Concerns that we had earlier about systematic errors arising from small, independent motions of the ring electrostatic plates have been addressed recently by the development of a system with monolithic magnets and electrostatic plates that contain two counter-rotating beams, in effect the time reversal equivalents of each other. We have therefore decided to pursue the frozen spin method, where a radial electric field is used to keep the longitudinally polarized deuteron spins almost aligned with their momentum (almost because we will let the spin precess very slowly with respect to the momentum vector for systematic error control). We have now developed a clear path towards a goal of $10^{-29}\,\mathrm{e}\cdot\mathrm{cm}$ in $\sim 10^7$ s of physics running time. Likewise, we have extensively studied the beam and spin dynamics systematic errors and concluded that they are manageable, below $10^{-29}\,\mathrm{e}\cdot\mathrm{cm}$. Since the polarimeter systematic errors are turning out to be the dominant ones, we have expanded the scope of the polarimeter detectors to provide much more information than we originally envisaged. We are taking a conservative approach, running very important polarimeter and spin manipulation tests at KVI (the Netherlands) and COSY (Germany) to test these concepts in detail and develop the final polarimeter system.

1.1 The frozen spin concept

We are proposing to store a longitudinally polarized deuteron beam of 1 GeV/c total momentum in a magnetic storage ring of 0.5 T. A particle in a magnetic storage ring with a vertical dipole magnetic field (B) will feel in its rest frame, in addition to the magnetic field, the presence of an electric field proportional to $\gamma\vec{v} \times \vec{B}$, with v its velocity and γ its Lorentz factor. The direction of the electric field is radial inward, always orthogonal to both the velocity and magnetic field vectors. If the particle has an EDM along its spin direction, this E-field will precess the particle spin into the vertical direction. This change of the vertical component of the beam polarization from early to late storage times is the signature of the EDM signal. The experiment is most sensitive when the deuteron spin is kept longitudinal, along the velocity vector, for the duration of the storage time. However, we will vary the horizontal precession rate in order to measure other polariation components and constrain our systematic errors. We plan to control the horizontal spin precession by using a radial E-field in the lab frame, produced by a pair of vertical capacitor plates. Without the radial E-field, the deuteron spin precesses slower than its momentum since the deuteron anomalous magnetic moment is negative ($a_d = -0.142$). This radial E-field is directed outwards, making the beam path longer for the same magnetic field and giving the deuteron spin a chance to catch up to its momentum. With the estimated spin coherence time of 10^3 s the spin precession due to an EDM of $10^{-29}\,\mathrm{e}\cdot\mathrm{cm}$ will produce a change in the vertical spin component of approximately $10\,\mu$rad during the storage time.

1.2 What is different from the 2004 proposal

The new concepts that make the goal of the present proposal two orders of magnitude better than our September 2004 proposal are:

1. The limiting error of $10^{-27}\,\mathrm{e}\cdot\mathrm{cm}$ in the 2004 proposal [5] was the time-dependent part of the spectrum of the average vertical electric field over the entire ring. Such a field effectively generates a radial B-field that can precess the deuteron polarization into the vertical direction and mimic an EDM signal. The statistical error, however, could have been achieved in one week's running time. We had planned to cancel the DC component of the E-field misalignment by clock-wise (CW) and counter-clock-wise (CCW) consecutive beam injections [5]. We are currently planning, in addition to consecutive CW and CCW injections, to have two independent rings located on top of each other, about 40 cm apart, with common vertical electric field plates. The beam in one ring will travel CW, while in the other ring it will travel CCW, ensuring the cancellation of the time-dependent variations of the vertical electric field caused by ground motion and/or temperature variations external to the vacuum chamber. We still plan to periodically reverse all magnetic fields, interchanging the places of the CW and CCW beams in order to retain this check on systematic errors. The counter-rotating beams in the two rings require dipole magnetic fields of opposite sign, which is made possible by a specially designed magnet (see Fig. 1) adapted to the dEDM needs. These kinds of magnets (a.k.a. common coil design magnets) have already been constructed at the magnet division of BNL [6] as well as at FNAL [7] and LBL [8].

2. Without electron cooling, the expected horizontal and vertical emittances of the beam injected into the EDM ring from the AGS are $> 10\pi$ mm mrad (95%, un-normalized) and the momentum spread is $> 2 \times 10^{-3}$ (full 95% spread). The calculated spin coherence time (SCT) of this beam would be $\sim 10^2$ s and its beam size in our ring would be 5 cm. We have decided to use electron cooling to reduce the

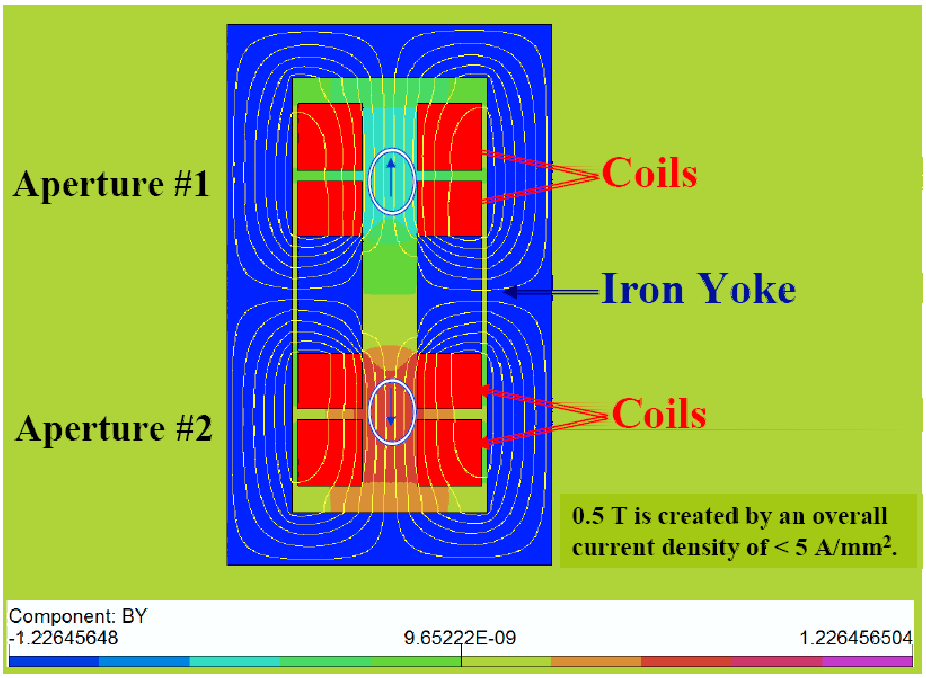

Figure 1: A schematic of the common coil magnet design (the horizontal and vertical scales are not the same). When the deuteron beam travels CW in aperture 1, the beam travels CCW in aperture 2.

horizontal emittance to 3π mm mrad (95%, absolute) and the momentum spread to 10^{-3} (full spread 95%). The SCT is then estimated to be better than $\sim 10^3$ s, while the horizontal beam size is going to be smaller than ± 1 cm. The experimental statistical error due to the expected increase in SCT (τ) goes as $1/\sqrt{\tau}$.

3. The statistical significance of the experiment scales roughly as the particle velocity times the dipole magnetic field strength, both of which depend on the strength of the radial electric field that can be safely applied in the ring to freeze the deuteron spin direction. Recent breakthroughs in the preparation of normal conducting surfaces have made possible the achievement of much higher electric fields [9]. Including the fact that the electric fields scale as $1/\sqrt{d}$ with d the distance between the electric field plates [10], we can now assume an electric field strength of 120 kV/cm. The recent improvements in the electric field strengths achieved with normal conducting cavities and the experience with the FNAL's Tevatron extended electrostatic separator system [11] give us confidence in our decision. The greater electric field value allows for a higher dipole magnetic field plus a higher deuteron beam velocity, enhancing the statistical strength of the experiment while making possible the reduction of the ring circumference by about a factor of two.

4. The main polarimeter systematic errors are related to deuteron beam position and angle changes as it strikes the analyzing target between the early and late stages of the storage time. We have extensively studied the extraction mechanism to ensure a smooth and uniform beam extraction onto the target from early to late times. In place of, or in addition to, the original segmented scintillator array envisioned

for the polarimeter, we are investigating TOF measurements using MRPC detectors with time resolution better than 50 ps [12] to reduce signal contamination by breakup protons and improve the polarimeter analyzing power. In addition, we are investigating the possibility of adding a micro-megas-TPC [13] detector capable of providing direction information on the incoming deuterons. When extrapolated back to target this tracking capability will yield information on the position where the projectile leaves the target, thus reducing systematic errors associated with early to late position stability issues.

2 Motivation for the Deuteron Electric Dipole Moment Experiment

Modern interest in particle and bound-state electric dipole moments began with the pioneering work of Norman Ramsey and his collaborators [1]. Their more than 50-year quest to find a non-zero neutron EDM anticipated parity (P) and time-reversal (T or CP) violation, necessary ingredients for the existence of an EDM, and paved the way for the current very restrictive bound [14]

$$|d_n| < 1.6 \times 10^{-26}\,\mathrm{e}\cdot\mathrm{cm} \quad (90\%\,\mathrm{CL}). \tag{1}$$

Over the years, improvements in the bound on d_n have been used to rule out or constrain various models of CP-violation, a testament to the power of null results.

Of course, we now know that P and T violation occurs in the $\mathrm{SU(3)_c \times SU(2)_L \times U(1)_Y}$ Standard Model via weak interactions and 3-generation quark mixing. So it is rather certain that all non-zero spin particles and bound-states possess EDMs, unless prevented by an exact symmetry. For example, a Majorana neutrino is self-conjugate under C and therefore cannot have an electric or magnetic dipole moment.

However, CP-violation due to quark mixing is small and only contributes to hadronic EDMs at the 3-loop level (leptonic EDMs at the 4-loop level). Hence, the Standard Model predictions for EDMs are currently unobservably small and will remain so for many years. We give in Table 1 current and planned bounds on the neutron, mercury, and Xenon EDMs (the three best constrained) and their neutron equivalent limits. We also give the planned deuteron nucleus limit and its neutron equivalent for comparison. We note that the bound for d_{Tl} is primarily used to provide a stringent upper limit on the electron EDM [15], d_e, via $d_{Tl} = \ -585\, d_e$

$$|d_e| < 1.5 \times 10^{-27}\,\mathrm{e}\cdot\mathrm{cm} \quad (90\%\,\mathrm{CL}). \tag{2}$$

CP-violation in the leptonic sector of the Standard Model occurs via neutrino masses and mixing. However, the loop-induced EDMs will be extremely small because of the tiny neutrino masses. Very rough estimates suggest $d_e^{leptonic} \leq 10^{-60}\,\mathrm{e}\cdot\mathrm{cm}$.

The unobservability of the SM EDM predictions provides us with an opportunity to search for new sources of CP-violation by continuing to improve EDM sensitivities via new experiments. The existence of those new sources is very well motivated for several reasons: 1) As pointed out by Sakharov [16], CP-violation is one of the necessary ingredients required to explain the matter-antimatter asymmetry of our universe. However, the Standard Model fails to explain this asymmetry by many orders of magnitude, thus pointing to a need for new, stronger sources of CP-violation. 2) New physics extensions to the Standard Model such as supersymmetry (SUSY) naturally introduce additional CP-violating phases that can contribute to ordinary particle EDMs at the 1-loop level. In fact, the existing bound on d_n already provides a severe constraint on supersymmetric models,

Table 1: **Current EDM limits in [e · cm], and long-term goals for the neutron, ^{199}Hg [17], ^{129}Xe, Deuteron nucleus, and their neutron equivalent limits. Screening [18] severely limits the sensitivity of ^{199}Hg, and ^{129}Xe, see text.**

Particle/Atom	Current EDM limit	Future Goal	$\sim d_n$ equivalent
Neutron	$< 1.6 \times 10^{-26}$	$\sim 10^{-28}$	10^{-28}
^{199}Hg	$< 2 \times 10^{-28}$	$\sim 2 \times 10^{-29}$	$10^{-25} - 10^{-26}$
^{129}Xe	$< 6 \times 10^{-27}$	$\sim 10^{-30} - 10^{-33}$	$10^{-26} - 10^{-29}$
Deuteron		$\sim 10^{-29}$	$3 \times 10^{-29} - 5 \times 10^{-31}$

requiring them to have very small phases or relatively high mass scales in those loops. An observation of any non-zero EDM in the forthcoming generation of experiments, which are expected to improve by several orders of magnitude, would find a natural explanation in supersymmetry and nicely complement direct collider searches for SUSY particles. The high payoff and strong motivation have made EDM experiments an exciting research frontier strongly endorsed by the atomic, nuclear and high energy physics communities.

To demonstrate the potential of the proposed new approach to EDM studies employing a charged particle storage ring, we compare d_n and d_D for some well-motivated new sources of CP-violation.

2.1 The QCD CP-violating parameter $\bar{\theta}$

Consider the $\bar{\theta}$ CP-violating parameter of QCD. It can be introduced into the Standard Model via appendages at some high scale which contribute to $\bar{\theta}$ via the quark mass matrix at the loop level. In the case of nucleons, one has the well-known relation

$$d_n \approx -d_p \approx 3 \times 10^{-16}\, \bar{\theta}\ \ \mathrm{e} \cdot \mathrm{cm}, \tag{3}$$

which implies the severe constraint

$$\bar{\theta} < 1 \times 10^{-10}. \tag{4}$$

In the case of the deuteron,

$$d_D \approx d_n + d_p + d_D^{nuclear}. \tag{5}$$

The nucleon contributions tend to cancel, but the nuclear contribution (which can be reliably calculated because of the deuteron's simple nuclear wavefunction [19, 20]) coming from an induced CP-violating pn interaction gives

$$\mid d_D(\bar{\theta}) \mid \approx 10^{-16}\, \bar{\theta}\, \mathrm{e} \cdot \mathrm{cm}. \tag{6}$$

At the level of $d_D \approx 10^{-29} \mathrm{e} \cdot \mathrm{cm}$ sensitivity, one probes $\bar{\theta}$ at 10^{-13}, three orders of magnitude beyond the current bound and about an order of magnitude beyond projected future d_n experimental goals. Since $\bar{\theta}$ contributes to d_n and d_D differently, it is clear that d_n and d_D experiments are highly complementary. Indeed the prediction

$$\mid d_D(\bar{\theta}) \mid / \mid d_n(\bar{\theta}) \mid \approx 1/3 \tag{7}$$

provides a beautiful check as to whether $\bar{\theta}$ is the source of the observed EDMs, should both d_n and d_D be measured.

2.2 Supersymmetry

Supersymmetry (SUSY) and the new particles associated with it (sparticles) are generally considered to be a very possible extension of the Standard Model. Generic predictions of such a scenario include a plethora of new particles which may be discovered at the LHC and new CP-violating phases that can generate EDMs for quarks, leptons and their associated bound-states. In fact, existing EDM bounds already severely constrain the parameter spaces of SUSY models. The next generation of EDM experiments has an extremely good chance of yielding positive results if SUSY turns out to be correct.

Below, we use SUSY as a way of comparing d_D with other EDM studies, primarily d_n, which is expected to be pushed to about $5 \times 10^{-28}\,\mathrm{e}\cdot\mathrm{cm}$ in the coming generation of experiments.

Following the work of Lebedev *et al.* [21] and the review article by Pospelov and Ritz [22], we note that SUSY loops give rise to ordinary quark EDMs, d_q, as well as quark-color EDMs, d_q^c. One finds

$$d_n \approx 1.4(d_d - 0.25 d_u) + 0.83 e(d_d^c + d_u^c) + 0.27 e(d_d^c - d_u^c), \tag{8}$$

where the color EDM contribution has been divided into isoscalar and isovector parts. Currently, the experimental bound on d_n suggests for color EDMs

$$|e(d_d^c + d_u^c)| \leq 2 \times 10^{-26}\,\mathrm{e}\cdot\mathrm{cm} \tag{9}$$

$$|e(d_d^c - d_u^c)| \leq 6 \times 10^{-26}\,\mathrm{e}\cdot\mathrm{cm}. \tag{10}$$

Almost an order of magnitude better bound on the isovector component comes from $^{199}\mathrm{H_g}$

$$|e(d_d^c - d_u^c)| \leq 2 \times 10^{-26}\,\mathrm{e}\cdot\mathrm{cm}. \tag{11}$$

Those constraints are already quite stringent. In the case of d_n, they are expected to be pushed by two orders of magnitude in the long term.

Now consider the SUSY prediction for the deuteron,

$$d_D \approx (d_d + d_u) + 6 e(d_d^c - d_u^c) - 0.2 e(d_d^c + d_u^c). \tag{12}$$

Comparing d_D with d_n in Eqs. (8, 12) illustrates a significant advantage of d_D. It is about 20 times more sensitive to the isovector component $e(d_d^c - d_u^c)$ than d_n because of the large two body, $I = 1$, pion exchange contribution. At a d_D sensitivity of $10^{-27}\,\mathrm{e}\cdot\mathrm{cm}$ (the old proposal goal), the bound on $e(d_d^c - d_u^c)$ in Eq. (10) is extended by 2 orders of magnitude and is more than an order of magnitude better than the ultimate goal of d_n experiments. It is much better than ^{199}Hg capabilities and, of course, much cleaner theoretically. When d_D is pushed to $10^{-29}\,\mathrm{e}\cdot\mathrm{cm}$ (our present goal), those constraints are extended by another two orders of magnitude, a remarkable capability. In the case of quark EDMs and the isoscalar combination $e(d_d^c + d_u^c)$, a sensitivity of d_D to $10^{-29}\,\mathrm{e}\cdot\mathrm{cm}$ is still more than an order of magnitude better than the best d_n expectations. It is clear that d_D is not only complementary to other EDM searches, but for some potential sources of EDMs, it is superior.

To put the above d_D sensitivities into perspective, we consider the results of Lebedev *et al.* [21] for some specific SUSY models. At $d_D \approx 10^{-27}\,\mathrm{e}\cdot\mathrm{cm}$, SUSY squark masses well beyond 10 TeV are probed, i.e., beyond LHC capabilities. At $10^{-29}\,\mathrm{e}\cdot\mathrm{cm}$, one explores scales extending beyond 100 TeV, a very impressive sensitivity.

2.3 Dimensional Analysis

To roughly estimate the scale of "New Physics" probed by EDM experiments, we often assume on dimensional grounds

$$d_i \approx \frac{m_i}{\Lambda^2} \mathrm{e} \sin\phi, \tag{13}$$

where m_i is the quark or lepton mass, $\sin\phi$ is the result of CP-violating phase, and Λ is the "New Physics" scale. For $m_q \sim 10$ MeV and $\sin\phi$ of order 1/2, one finds

$$d_D \sim 10^{-22} \left(\frac{1\,\mathrm{TeV}}{\Lambda}\right)^2 \mathrm{e}\cdot\mathrm{cm}. \tag{14}$$

So, $d_D \sim 10^{-29}\,\mathrm{e}\cdot\mathrm{cm}$ sensitivity probes $\Lambda \sim 3000$ TeV. More realistically, the d_i generally results from a quantum loop effect and there is a further $g^2/16\pi^2 \sim 1/100$ suppression. So, for example, in supersymmetry one might expect

$$d_D \sim 10^{-24} \left(\frac{1\,\mathrm{TeV}}{M_{\mathrm{SUSY}}}\right)^2 \sin\phi\,\mathrm{e}\cdot\mathrm{cm}. \tag{15}$$

In such a theory, with $M_{SUSY} \leq 1$ TeV, $\sin\phi$ would have to be very small, $\leq 10^{-5}$ if a $d_D \geq 10^{-29}\,\mathrm{e}\cdot\mathrm{cm}$ were not observed. Of course, one hopes that the LHC may actually observe squarks in the TeV or lower range and that $\sin\phi \geq 10^{-5}$. If that is the case, d_D will provide precise EDM measurements that will unveil their CP-violating nature and perhaps help to explain the matter-antimatter asymmetry of our universe.

Other new models of CP-violation from Left-Right symmetric gauge theories, additional Higgs scalars, etc. can also be studied using EDM experiments. In such cases, d_D at $10^{-27}\,\mathrm{e}\cdot\mathrm{cm}$ is competitive with or better than other EDM measurements, while at $10^{-29}\,\mathrm{e}\cdot\mathrm{cm}$ it is our best hope for finding new sources of CP-violation. Couple that sensitivity with the relative theoretical simplicity of the deuteron wavefunction for calculating d_D and it becomes clear that the deuteron EDM holds great discovery potential and the storage ring method should therefore be vigorously pursued.

3 Concept of Experiment

3.1 Overview of the Experimental Technique

In our proposed experiment, the EDM of D^+, the bare deuteron nucleus is directly probed using a storage ring technique which has the potential to increase the sensitivity of EDM measurements by several orders of magnitude. Longitudinally polarized deuterons are first injected into a storage ring. During the storage time, we probe the spin precession in both the "horizontal" and "vertical" directions by polarimetry, detecting deuterons scattered by solid carbon targets. For a particle at rest, an EDM couples to the electric field and a magnetic moment couples to the magnetic field. Since a relativistic particle in a magnetic storage ring feels both magnetic and electric fields in its rest frame, its spin precession vector will be modified by the presence of an EDM. This was recognized early on [23] and this method was applied to set limits on the muon EDM [24]. The EDM signal is a change in the "vertical" polarization, with time given by

$$\Delta P_V = P\,\frac{\omega_{edm}}{\Omega}\,\sin(\Omega t + \theta_0), \qquad \Omega = \sqrt{\omega_{edm}^2 + \omega_a^2}, \tag{16}$$

where P is the polarization of the particle beam, and ω_a, ω_{edm} are the precession frequencies arising from the magnetic and electric dipole moments, respectively. ω_a is the

"horizontal" precession frequency measured in g-2 experiments. ω_{edm} is a "vertical precession" which would tip the usual g-2 precession out of the horizontal plane. In our experiment, we maximize the change in the "vertical" polarization during beam storage by applying a radial E-field [2, 25], and reduce ω_a by a factor of more than 10^9. Then $\Omega\, t < 1$ at all times up to 10^3 s, and, for small θ_0, the term $\sin(\Omega t + \theta_0) \simeq \Omega\, t + \theta_0$. Therefore $\Delta P_V(t) \simeq P\, \omega_{EDM}\, t$, i.e., canceling ω_a to $\geq 10^9$ amplifies the maximum value of $\Delta P_V(t)$ by 10^9.

The storage ring provides a clean environment with intense, highly polarized, and stable beams of low emittance. The dominant systematic errors of the traditional neutral particle EDM search techniques are absent, or highly suppressed. First we discuss the problems inherent in the traditional neutral particle EDM experimental method, and then introduce the new storage ring method. The spin precession for a particle at rest, $\vec{v} = 0$, is:

$$\frac{d\vec{S}}{dt} = \mu\hat{S} \times \vec{B} + d\hat{S} \times \vec{E}, \tag{17}$$

where the magnetic moment $\mu = ge/2mc$, d is the electric dipole moment, $\hat{S} = \vec{S}/S$, with S the spin quantum number. For the neutron, e/m of the proton is used; and $g_n = -3.8$. Neutron EDM experiments have been ongoing since the 1950s [26]. The experiments have been performed in a weak magnetic field, typically 1 μT, and a strong electric field, typically 2 MV/m. The spin precession frequency is measured with the electric field parallel and anti-parallel to the magnetic field. A change in the measured spin precession frequency would be evidence for an EDM.

A systematic error can originate from any stray magnetic field, such as one caused by leakage currents from the electric field electrodes that changes sign when the electric field is flipped. In a real neutral particle EDM experiment with $|\vec{v}| \ll c$, the spin precession is given by

$$\frac{d\vec{S}}{dt} = \mu\hat{S} \times \left(\vec{B} - \vec{v} \times \vec{E}\right) + d\hat{S} \times \left(\vec{E} + \vec{v} \times \vec{B}\right). \tag{18}$$

The $\mu(\hat{S} \times (\vec{v} \times \vec{E}))$ term represents a systematic error in the EDM search since this term, like the EDM precession term, changes sign when the electric field changes sign. Note that the $d(\hat{S} \times (\vec{v} \times \vec{B}))$ term increases the EDM signal, but it is negligible compared to the electric field term.

Next we discuss the situation for a relativistic particle in a storage ring [27] where there are both magnetic and electric fields. The spin precession due to the magnetic dipole moment is:

$$\frac{d\vec{S}}{dt} = \frac{e}{m}\vec{S} \times \left[\left(a + \frac{1}{\gamma}\right)\vec{B} - a\frac{\gamma}{\gamma+1}\left(\vec{\beta}\cdot\vec{B}\right)\vec{\beta} - \left(\frac{g}{2} - \frac{\gamma}{\gamma+1}\right)\frac{\vec{\beta}\times\vec{E}}{c}\right], \tag{19}$$

where $a = (g-2)/2$ is the anomalous magnetic moment. The spin precession due to the electric dipole moment is simply:

$$\frac{d\vec{S}}{dt} = d\left[\hat{S} \times \left(c\vec{\beta} \times \vec{B} + \vec{E}\right)\right]. \tag{20}$$

The $d\,\hat{S} \times \vec{E}$ term can be neglected in the above equation, since this change in the EDM signal is small compared to the magnetic field term. The spin precession due to the electric dipole moment is about the $\vec{\beta} \times \vec{B}$ vector.

For the simple case of $\vec{\beta} \cdot \vec{B} = \vec{\beta} \cdot \vec{E} = 0$, the precession of the spin direction relative to the momentum direction is given by $\vec{\omega} = \vec{\omega}_a + \vec{\omega}_{edm}$, where

$$\vec{\omega}_a = \frac{e}{m} \left[a\vec{B} + \left(\frac{1}{\gamma^2 - 1} - a \right) \frac{\vec{\beta} \times \vec{E}}{c} \right] \tag{21}$$

is the rotation about the vertical ($\vec{B}$-field direction) direction that arises because there is an anomalous part to the magnetic moment. The frequency about the radial direction (for a spin one particle $S = 1$) is

$$\vec{\omega}_{edm} = d \, \frac{c}{\hbar S} \left(\frac{\vec{E}}{c} + \vec{\beta} \times \vec{B} \right), \tag{22}$$

which comes from the torque produced on the EDM. The EDM signal is an increasingly vertical polarization produced by a non-vanishing ω_{edm} precession. The change in the vertical polarization with time is given in Eq. (16). Thus, it behooves us to minimize ω_a, although for systematic error management ω_a should be small but not zero. This can be done by applying a radial electric field of magnitude

$$E_r = \frac{aBc\beta\gamma^2}{1 - a\beta^2\gamma^2} \simeq aBc\beta\gamma^2 \tag{23}$$

to cancel the $a\vec{B}$ contribution to ω_a in Eq. (21) [2, 25]. A sensitive EDM search requires large electric fields and particles with a small anomalous moment.

Unfortunately, there are no particles with $a = 0$. Leptons have $a \simeq 0.001$. The electron imposes difficulties using the storage ring technique since it generates a large amount of synchrotron radiation, which introduces an additional systematic error: an electron beam in a storage ring develops a polarization component along the direction of the magnetic field vector. The situation is much better for the muon since synchrotron radiation intensity falls as $1/m^4$. An LOI has been submitted to JPARC [28] for a muon EDM experiment at the level of $10^{-24}\,\mathrm{e} \cdot \mathrm{cm}$ statistical and orders of magnitude lower systematic error. The statistical error is large because of the difficulty of obtaining a sufficient flux of stored muons; the muon beam derives from a secondary pion beam and is created with very large emittance. Its lifetime also limits the time for observing the EDM precession. The challenge of a MW proton beam creating an intense muon beam means that this experiment is at least one decade away from physical realization. Thus other cases that can reach the same level of sensitivity in a shorter time are preferred.

The deuteron is an ideal candidate. It has a small anomaly, $a = -0.143$. Intense, low-emittance beams with high polarization and efficient polarimeters are readily available. We are proposing here a search for the deuteron EDM with statistical error of $10^{-29}\,\mathrm{e} \cdot \mathrm{cm}$ and systematic error of less than $10^{-29}\,\mathrm{e} \cdot \mathrm{cm}$.

The EDM systematic error due to a weak magnetic field induced by leakage currents from the electric field electrodes is negligible since the storage ring magnetic field is strong ($\simeq 0.5$ T), not weak ($\simeq 10^{-6}$ T), as in the neutral beam EDM experiments. Furthermore, in the storage ring EDM search, the $\vec{v} \times \vec{E}$ precession term is not a systematic error, but rather a tool to control the $g - 2$ precession rate to increase the statistical sensitivity to the EDM. In order to control systematic errors, the $g - 2$ precession rate is varied, as discussed later.

We have extensively studied spin dynamics systematic errors [2] and have found only one first-order spin dynamics systematic effect for the Storage Ring EDM experiment: if

there is a non-zero average value for the vertical component of the electric field, $\langle E_V \rangle \equiv \langle \vec{E} \cdot \vec{B} \rangle / B \neq 0$, then the spin will precess about the radial direction:

$$\omega_{syst} \simeq \frac{\mu \langle E_V \rangle}{\beta c \gamma^2}. \tag{24}$$

This effect, relative to the EDM effect, changes sign when we inject the beam clock-wise (CW) vs. counter-clockwise (CCW) into the ring. This can be seen from Eqs. (21) and (22). In going from CW to CCW, $\vec{\beta} \to -\vec{\beta}$, $\vec{B} \to -\vec{B}$, and $\vec{E} \to \vec{E}$; therefore $\vec{\omega}_a$, and thus ω_{syst}, changes sign, while ω_{edm} does not. Thus, conceptually, the EDM signal is separated from false signals in a comparison of the measured deuteron spin precession rates about the $\vec{\beta} \times \vec{B}$ direction when we inject CW vs. CCW. The ratio of the spin precession (due to the vertical electric field) to the EDM spin precession, which needs to be minimized in the design of the experiment, is given by

$$R = \frac{a\,\mu \langle E_V \rangle}{d \beta c E}\ . \tag{25}$$

We have chosen for a storage ring conceptual design $p_D = 1$ GeV/c or $\beta = 0.5$. A larger value of β would reduce the ratio R; however, the ring cost would increase. The electric field value $E \simeq \pm 120\,\mathrm{kV}/2\,\mathrm{cm}$ results in $B \simeq 0.5$ T.

3.2 Polarimeter Design Considerations

The signal of an EDM is a changing vertical component of the stored beam's polarization. Measuring such a change requires continuous monitoring of that component during the time that the stored beam is circulating in the ring, and looking for a particular time dependence associated with the lifetime of the stored beam. The most efficient polarization monitor is scattering from a nucleus where the sensitivity to the amount of vertical polarization is given by the spin-orbit part of the strong nuclear interaction between the deuteron and the target nucleus. Thus, the polarimeter must be able to sample the stored beam over time and, with high efficiency and extremely low systematic error, scatter deuterons (or other particles) into angles where they are easily detected using standard particle tracking technology.

In this section, we begin with a brief discussion of the design requirements for the polarimeter and the ways that we are investigating the management of systematic errors due to position and angle misalignments of the beam. These errors are the subject of a proposal that was submitted to the Program Advisory Committee for the Cooler Synchrotron (COSY) storage ring at the Forschungszentrum-Jülich. Eight weeks of beam time have been approved for proof-of-principle studies and the collection of more deuteron-carbon scattering and reaction data to be used for polarimeter simulations. At this time the first run is scheduled for June, 2008, to set up new electronics for our work and to investigate issues surrounding efficient running of an EDM polarimeter. After discussing these issues, we review the way in which we plan to run with the EDM storage ring, and show a simple illustration of the data we expect to obtain.

Since 2004, we have also had approved beam time for polarized deuterons at the KVI cyclotron in Groningen. At first, this time was used for the measurement of a broad range of elastic scattering and reaction products that we expected to see in our final EDM polarimeter. More recently, data have been taken on the sensitivity of deuteron-carbon reactions to position and angle errors in the beam. These results will be discussed below.

3.2.1 Polarimeter Design

In the region below 250 MeV, the best sensitivity to vector polarization is forward-angle elastic scattering. In general, this sensitivity is described by the vector and tensor polarizations that are possible using a spin-1 beam along with their analyzing powers that contain the sensitivity of the scattering or reaction process to those polarizations. This sensitivity is given by:

$$\sigma_{pol} = \sigma_{unpol} \ (1 + 2 \ it_{11} \ iT_{11} + t_{20} \ T_{20} + 2 \ t_{21} \ T_{21} + 2 \ t_{22} \ T_{22}) \,, \tag{26}$$

where the small t_{kq} are the beam polarizations and the large T_{kq} are the associated analyzing powers. The EDM signal will appear as a non-zero value of it_{11} (in the vertical direction). So we need to find a process for which iT_{11} is as large as possible consistent with also having a large cross section for efficiency. The most forward analyzing power maximum in deuteron elastic scattering from carbon appears to be the best choice. Figure (2) shows measurements of deuteron elastic scattering from RIKEN at 270 MeV [29]. The data collection limits are expected to start at angles as small as 5° and extend out

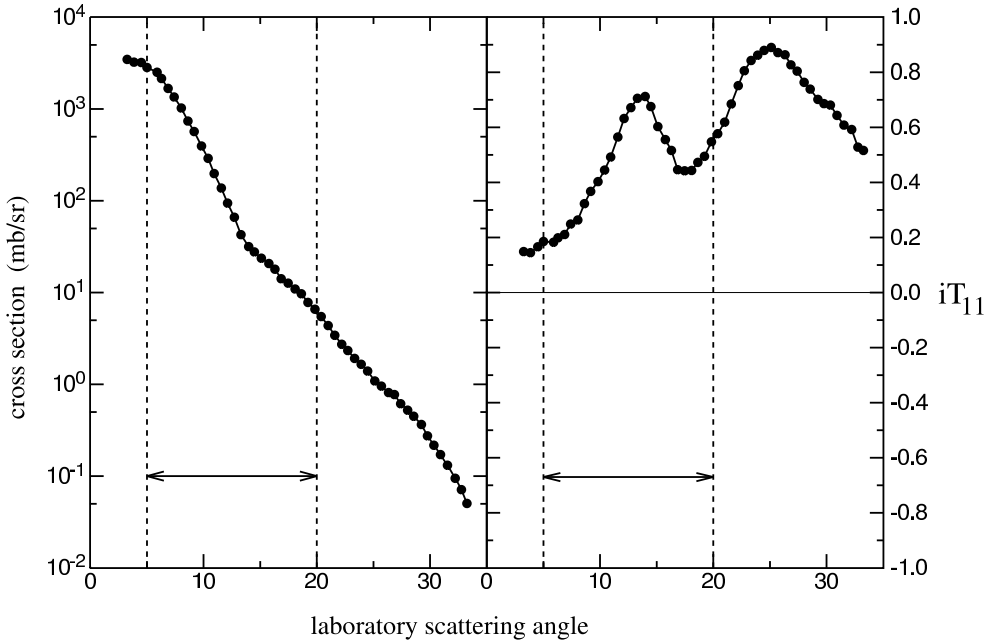

Figure 2: Deuteron elastic cross section and analyzing power at 270 MeV from carbon [29]. The dashed lines indicate the preferred acceptance limits for an EDM polarimeter.

to and past 20°. In this range, the vector analyzing power reaches its first peak. Here the large cross section makes this scattering an efficient way to determine deuteron vector polarization. While the interference oscillations may differ, most reactions leading to deuterons or protons with low reaction Q-values also have positive analyzing powers in this angle range and could usefully be included as a part of the acceptable events, thus loosening the requirements on energy resolution. Measurements made at the KVI at 76 and 113 MeV (as a part of the preparation for this experiment) show that the analyzing power of protons from deuteron breakup has almost no spin sensitivity, in particular near

the peak of the breakup cross section distribution in outgoing energy. Excluding these events from the polarimeter acceptance will improve performance.

A critical parameter in the design of the polarimeter is the accumulation of a large statistical sample throughout the beam store. Compared to the extremely thin targets that typically are used to intersect a stored beam, it is essential that as far as possible each deuteron traverses the maximum amount of carbon material (between 4 and 6 cm) for each encounter with the target. We propose to place a target with this thickness and cut as a smooth edge near the beam. If it is close enough to the beam, this edge will become the defining aperture for the entire EDM storage ring. In this case, any deuterons lost from the ring due to interactions with the background gas in the vacuum will eventually be lost from the stored beam by hitting this target. Targets of comparable thickness have been used at Saturne for measuring deuteron polarization ([30] and references therein). Polarimeter efficiencies of a few percent characterize this work.

Beam time has been approved for June 2008 for COSY-Jülich to investigate what is the best configuration for such a target. Carbon samples in the form of both a tube (with the beam going through the center) and a 2-mm thick edge that comes close to the beam on one side have been prepared. The edge target will eventually intercept all deuterons with a betatron amplitude that exceeds the distance from the central closed orbit to the edge. Thus, effectively all of the beam can eventually be removed on such a target.

The emittance of the beam will slowly increase due mainly to Rutherford scattering with the residual gas atoms in the vacuum chamber. Calculations which include both large angle single and multiple small angle collisions indicate that 10^{-11} Bar vacuum pressure will give the desired rate on the Carbon target. For the tests at COSY, we plan to have available the ANKE cluster jet target, so that controlled studies can be made of the loss rates and beam lifetime.

The efficiency of this scheme depends on the way in which the front face of the carbon target is illuminated. Single Coulomb scattering from residual gas may produce average depths of a few millimeters, more than enough to prevent sideways re-emergence of the beam from multiple scattering. Deuterons that enter close to the edge may exit through the surface close to the beam or produce breakup protons, leading to events with an energy higher than those that must pass through the full target thickness. This may increase the fraction of events composed of protons from deuteron breakup. The work at COSY will provide data on this process. The tube target was intended to provide uniform coverage from all sides of the beam, but creates difficulties if, during the store, the beam becomes unbalanced on the left and right sides. The edge target solves this problem since all events emerge from one point, but with the feature that left and right exposure to the inner target face is asymmetric. Systematic polarization errors from both will be measured at COSY.

3.2.2 Polarimeter errors

We plan to have multiple deuteron beam bunches circulating in the EDM ring at the same time with opposite states of polarization. This is one of the most common ways of rejecting systematic errors due to detector acceptance differences. If L and R denote the counting rates in the left and right detectors, the vector asymmetry for $+$ and $-$ polariation states is given by

$$\epsilon_{LR} = 2\ it_{11}\ iT_{11} = \frac{r-1}{r+1} \qquad r^2 = \frac{L_+ R_-}{L_- R_+}. \tag{27}$$

If the spin-sensitive scattering process is nominally symmetric for perfect beam alignment in the polarimeter, then this scheme cancels first-order errors from beam misalignment in position and angle. However, second-order effects exist. If the misalignment

is characterized by an angle θ and the polarization up-and-down bunches have different polarizations (denoted by $u = p_+ + p_-$ where $p_- < 0$), then the asymmetry is changed by

$$\epsilon \leftarrow \epsilon + \frac{1}{1-\epsilon^2}\left[\epsilon^3 u^2 + 2\epsilon^2 \frac{\partial i T_{11}}{i T_{11} \partial \theta} u\theta + \epsilon\left(\frac{\partial^2 i T_{11}}{i T_{11} \partial \theta^2}(1-\epsilon^2) - \left(\frac{\partial i T_{11}}{i T_{11} \partial \theta}\right)^2 \epsilon^2\right)\theta^2\right]. \quad (28)$$

Here the ϵ on the right hand side is likely not the EDM signal but a steady background that is a residual of the beam polarization preparation process (and which will probably not be set to zero better than a few parts per thousand). The most severe constraints on beam stability early to late in the store are generated by the θ^2 term. Using values of the logarithmic derivatives of the analyzing power based on elastic scattering, keeping the errors below 10^{-29} e$\cdot$cm requires angle shifts less than 0.1 mrad and position shifts less than 0.1 mm for a 1-m deep polarimeter construction. For the tube target design, a position shift can amplify such systematic effects since it modulates the illumination of the left and right sides of the opening. The edge target eliminates this ambiguity, but has the problem that the scattering is not nominally left-right symmetric, a source of first-order errors. These effects will be investigated in more detail at COSY.

Error studies using the In-Beam Polarimeter (IBP) at the KVI cyclotron in Groningen looked specifically at the possibility to measure the second-order errors of Eq. (28). The results for a deuteron scattering angle of 18° are shown in Fig. (3). The quality of agreement in both curvature (θ^2 term) and slope ($u\theta$ term) is excellent and confirms the use of such a Taylor series analysis for understanding quantitatively the polarimeter errors. Development of the models on which these predictions were based is continuing, and eventually will be added to simulations of the EDM target configuration to make much more precise predictions of polarimeter performance.

One consequence of this study for the design of the polarimeter is the necessity, if we use a tube target, of monitoring the relative flux from all sides of the target. One possible detector design involves placing segmented plastic scintillators that cover the range of scattering angles from 10° to 20° behind iron absorbers [31] (1.5 − 2.0 cm), a scheme that was used in this energy range for deuteron polarization transfer measurements at Saturne. We are considering replacing this concept with a micro-megas-TPC [13] whose tracking ability would allow us to know about changes that would alter the illumination of the sides of the tube. If we feel that we need the constraints of an edge target, then it will become necessary to distinguish breakup protons from deuterons, a job that can be addressed using dE/dx measurements or TOF measurements with a multi-resistive plate chamber [12].

For the EDM storage ring, a polarimeter could be located in one of the two straight sections between quadrupole magnets. A target placed near the exit of one quadrupole would allow scattered particles to emerge from a 5-cm diameter beam pipe and pass into a detector before reaching the next quadrupole.

For the design of the EDM polarimeter, additional broad range data covering deuteron scattering and breakup are needed at energies above those available at the KVI. For this purpose, the proposal to COSY-Jülich also requested time on the WASA detector using a solid carbon target (not yet available) to measure the necessary spectra and their spin dependence at a variety of energies up to 250 MeV. This time is approved but not scheduled awaiting work on the design of a solid target assembly to operate with the WASA detector.

3.2.3 Running cycle

In the actual search for an EDM, vertically polarized deuteron beams will be loaded into both the CW and CCW storage rings. Bunching will be managed by an RF cavity.

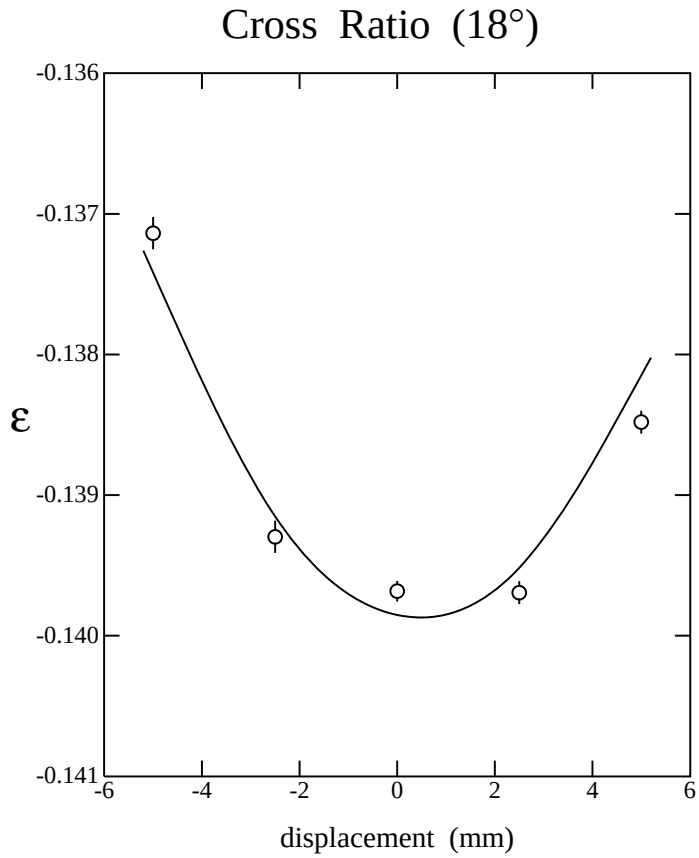

Figure 3: Measurements of the change in left-right asymmetry as the target position is moved horizontally. The solid line is an *a priori* prediction based on the older scattering measurements at 113 MeV. The curve has been offset vertically to match the average asymmetry. The errors shown are statistical only and do not include effects due to the setup of the beam position shifts and other systematic considerations.

Subsequent bunches will have opposite polarization directions. Sometimes unpolarized control bunches will be used.

Once all beams are in the ring, solenoids along each ring will be turned on for a short time to precess these polarizations into the horizontal plane. The solenoids need not be operated at some frequency since, with the electric field, the $g-2$ precession will be negligable during the time that they are on. The completion of this step starts the running for that store. The polarimeter will operate continuously, monitoring the vector (and tensor) polarization components. The beam will be dumped when either the polarization is too low or the current is too low. The process will be repeated, but with the magnetic fields of the storage rings reversed (leaving the electric fields intact). The injection directions for the upper and lower rings will be exchanged, reversing the roles of CW and CCW.

Data from all parts of this running cycle will be combined to cancel contributions from systematic errors that do not flip with polarization state or have a time-reversal conserving dependence on the direction of the beam in the storage rings.

3.2.4 Producing a Polarized Beam and What is Observed

A polarized ion source for spin-one deuteron beams changes the fraction, f_1, f_0, or f_{-1}, of the beam that is in each of the three magnetic substates away from the unpolarized values of $f_1 = f_0 = f_{-1} = 1/3$. This can produce a vector polarization ($p_V = f_1 - f_{-1}$) and/or a tensor polarization ($p_T = 1 - 3f_0$) with respect to the orientation of the quantization axis established by the magnetic field in the ion source. High statistical sensitivity to the EDM requires that the vector polarization be as large as possible, or $f_1 \sim 1$. In this case both f_0 and f_{-1} are close to zero and there is also a maximally large and positive tensor polarization. One secondary effect of this choice is that when the projection of the beam quantization axis onto the plane of the storage ring does not lie along a coordinate axis (either x or z), a left-right asymmetry is introduced that must be distinguished from an EDM signal.

A thorough knowledge of the polarization components requires that we detect particles at a variety of angles (θ, ϕ) where θ is the polar angle measured from the momentum direction and ϕ is the azimuthal angle that starts from the left (facing along the beam momentum) in the $g-2$ precession plane and advancing in the clockwise direction. The orientation at the scattering target of the quantization axis produced by the polarized ion source is a result of the cumulative effect of the transport line and ring electromagnetic fields. Its orientation when it reaches the polarimeter target is specified by a second set of spherical angles (ξ, ψ) with respect to the same reference frame. For a particle emerging from the target at (θ, ϕ), the differential cross section is modified according to

$$\sigma(\theta,\phi) = \sigma_{unp}(\theta)\,[1 + 2\ it_{11}\ iT_{11}(\theta) + t_{20}\ T_{20}(\theta) + 2\ t_{21}\ T_{21}(\theta) + 2\ t_{22}\ T_{22}(\theta)]\,, \qquad (29)$$

where the $T_{kq}(\theta)$ are the analyzing powers of rank k ($k = 1$ is vector, $k = 2$ is tensor) and the t_{kq} are the corresponding beam polarizations that are given by

$$\begin{aligned} it_{11} &= \frac{\sqrt{3}}{2}\ p_V\ \sin\xi\ \sin(\psi-\phi) \\ t_{20} &= \frac{1}{2\sqrt{2}}\ p_T\ (3\cos^2\xi - 1) \\ t_{21} &= -\sqrt{\frac{3}{2}}\ p_T\ \sin\xi\ \cos\xi\ \cos(\psi-\phi) \\ t_{22} &= \frac{\sqrt{3}}{4}\ p_T\ \sin^2\xi\ \cos 2(\psi-\phi)\ . \end{aligned} \qquad (30)$$

The small vertical spin component that signals the presence of an intrinsic EDM appears as a left-right asymmetry through the $it_{11}iT_{11}$ term in Eq. (29) because p_V is large (~ 0.8) and $\psi - \phi = \pm\pi/2$ maximizes $\sin(\psi - \phi)$. This happens with the opposite sign on the left and right sides of the beam when the vertical component makes $\psi = \pm\pi/2$. Such an asymmetry can also arise through the $t_{21}T_{21}$ term if $p_T \neq 0$ and $\psi - \phi \sim 0$ or π. This situation arises naturally if the anomalous precession is not cancelled to an extremely high precision (less than 1 part in 10^{12} for 10^{-29} e·cm) that we in practice cannot achieve. However, if the deuteron in-plane polarization were allowed to precess slowly (by virtue of the fact that the sizes of the electric and magnetic fields are slightly different from the condition that freezes the polarization direction) with an angular velocity ω_a, the precession can be tracked and used to separate various contributions to the polarization measurement that are unrelated to an EDM, exposing the signal of interest. One can distinguish the EDM and t_{21} effects by measuring the vertical polarization component as a function of time. An analysis would separate the $\sin\xi$ from the $\sin\xi\cos\xi = (\sin 2\xi)/2$ dependence provided ξ was allowed to vary by a large enough angle such as π. In general,

there are a number of systematic sources of a left-right asymmetry, such as a vertical polarization in the injected beam, misalignments of the beam at the polarimeter, non-linear detector response, and magnetic field errors that produce non-commuting rotations as the beam circles the ring. The time-dependent analysis is crucial for extracting the $\sin\xi$ term associated with an EDM.

In addition to the changes in the observed polarization that are a consequence of ξ changing with time, we expect that the magnitude of the polarization itself will be declining exponentially as the deuterons within the beam slowly respond to different phase space conditions within the beam. Since the tensor polarization reverses after a quantization axis rotation of only $\pi/2$ rather that π, it will depolarize with a time constant that is half of the vector polarization time constant [32].

The polarimeter data from the EDM search will consist of a set of deuteron polarization components measured as a function of the time during the store while the polarization slowly precesses ($\omega_a \neq 0$). Three possible asymmetries are shown in Fig. (4) as a function of time in a 100-second beam store (top panels) in which the polarization coherence time is 200 s. Initially, the beam polarization is sideways (along the positive x axis, maximizing ϵ_{DU}) and the rotation begins toward the beam momentum direction. The left-right asymmetry ϵ_{LR} is only one of the observed polarization components. The largest is the down-up asymmetry ϵ_{DU} ($2it_{11}\langle iT_{11}\rangle > 0.5$) from the horizontal component of the vector polarization. The t_{22} tensor polarization produces another asymmetry ϵ_{22} that makes the sum of down and up rates different from the sum of left and right rates. This asymmetry is at a level of 0.03. There is a tensor contribution to the left-right (EDM) asymmetry that comes from the t_{21} beam polarization. This asymmetry is at the level of 0.02. This signal has a period in ξ that is half that of the EDM signal (greatly enhanced in this simulation and shown as the short dashed line in the upper middle panel), a feature that may be used to separate this contribution.

An analysis of the EDM data requires the use of a model that carries these features as well as others not covered here. Thus, the EDM signal is more than a simple asymmetry. It is (1) a time-varying polarization component associated with $\sin\xi$ whose maximum size (2) varies as $\omega_{edm}/\sqrt{\omega_{edm}^2+\omega_a^2}$ and (3) has the correct behavior with respect to various reversals that are built into the running plan. These reversals include change of the vector polarization sign (by solenoid field change or source RF transition), change of beam revolution direction (CW or CCW), and change of sign of the uncancelled anomalous precession (ω_a). In addition, the time dependence of the EDM signal must be the integral of the longitudinal component of the vector polarization, beginning with zero as the store starts. For measurements which differ only in the sign of ω_a, time reversal violation requires that the EDM signal also change sign, a feature that separates it from many other systematic effects. This can be deduced in the presence of depolarization by using the tensor contributions to the asymmetry to separate different components and to locate the direction of the vector polarization in space. Note that as the beam depolarizes, this EDM-related oscillation also grows smaller with time and in this case does not ever cross zero except at the start.

Inherent in this scheme is the use of down-up and tensor asymmetries to set the time when the polarization vector passes above or below the momentum direction so that the zero point for ξ is known. In cases where ω_a is not constant with time, looking at the correlations between asymmetries can yield EDM signatures that are independent of ω_a. The bottom panels of Fig. (4) show two correlations in which the signal without an EDM piece is shown by the long-dashed lines. For ϵ_{DU} versus ϵ_{LR}, the EDM produces a tilt of the pattern. (The absolute horizontal shift is a function of when the data-taking starts and is not in itself an EDM effect.) Likewise, similar horizontal shifts are present in the

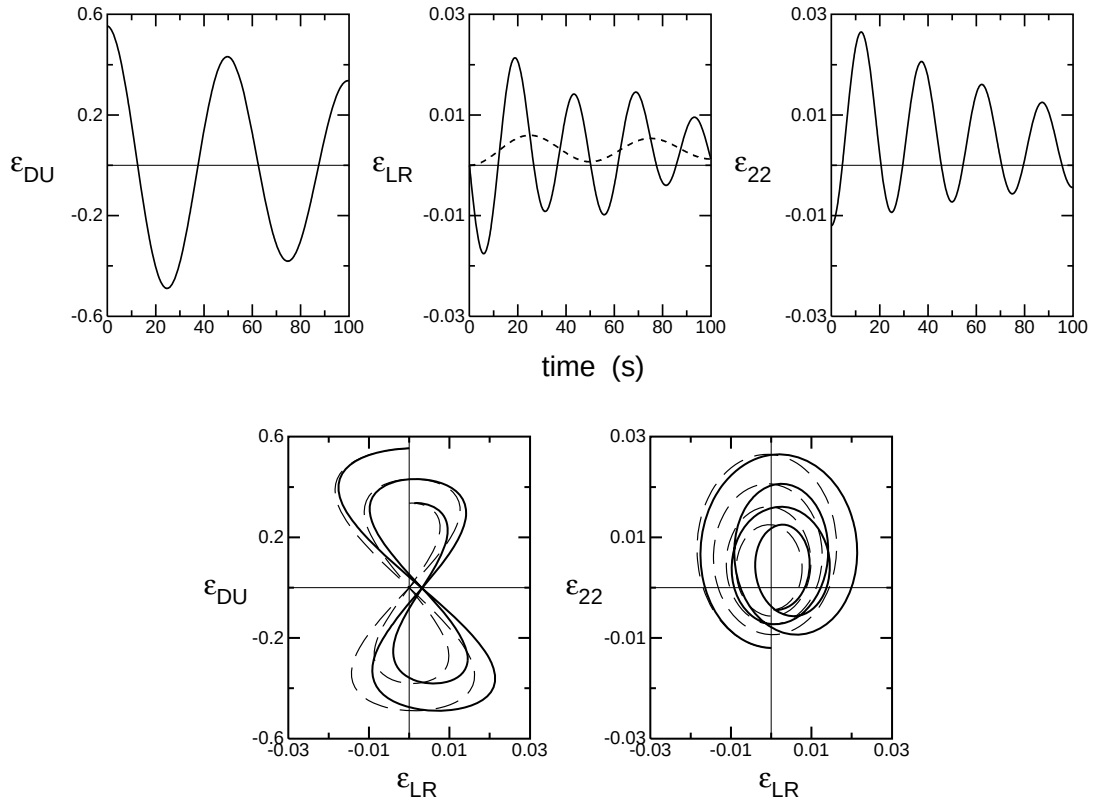

Figure 4: The polarimeter asymmetries as a function of time in the beam store. The short dashed curve in the upper middle panel represents the EDM signal alone. The long dashed correlation curves in the lower panels contain no EDM effect.

correlation of ϵ_{22} with ϵ_{LR} and may be used to confirm any EDM observation. Without an EDM, a smooth spiral results.

For a sensitivity to an EDM at the level of 10^{-29} e·cm, we need to detect a change in ϵ_{LR} of about 5×10^{-6} for the smallest practical values of ω_a.

3.3 Statistical Accuracy

An estimate of the time required to reach a sensitivity of $10^{-29}\,\mathrm{e}\cdot\mathrm{cm}$ must consider that the beam itself is being used up and the polarization is decreasing exponentially. A simple estimate can be made for polarization that is initially fixed along the momentum of the beam. An optimization gives the best result for a measurement time that is equal to the polarization lifetime, and a beam lifetime that is half of the polarization lifetime. In this case the one standard deviation error on d is

$$\sigma_d \approx \frac{8\hbar}{\sqrt{\tau_p}\,(\beta c B_V - E_R)\;\imath t_{11}\langle \imath T_{11}\rangle\;\sqrt{N_c f T_{tot}}}\ . \tag{31}$$

For a ring with momentum $p = 1$ GeV/c and polarization lifetime $\tau_p = 10^3$ s, we use $E_R = 12$ MV/m, $B_V = 0.5$ T, and $N_c = 2 \times 10^{11}$ deuterons/fill. The polarimeter has an efficiency of $f = 0.01$ and an effective asymmetry of $2\,\imath t_{11}\langle \imath T_{11}\rangle = 0.36$. The time needed to reach an error of $\sigma_d = 10^{-29}\,\mathrm{e}\cdot\mathrm{cm}$ is about $T_{tot} = 10^7$ s.

We request running time for 6 months for commissioning the ring and another 6 months for the first measurement. Most of the first 6-months' running time will go toward the investigation of systematic errors. In particular, measurements will be made at multiple

values of ω_a to learn whether the $\sin\xi$ Fourier component has a strength that varies as $\omega_{edm}/\sqrt{\omega_{edm}^2+\omega_a^2}$. We wish to take this running time over a span of two years.

With 10^{11} deuterons/fill/ring, the maximum possible polarimeter rate is $\sim 10^8$ events/s with 100% detection efficiency. We will use either current-mode sampling as the method of detector readout or single particle detection. The current mode has worked well for recent parity-violation experiments where the asymmetry associated with the signal is small [33]. The alternative method we are investigating is to use single particle detection with a detector that can operate well in a high-rate environment, such as the micro-megas [13].

4 Deuteron Storage Ring

4.1 Lattice Design Considerations

The conceptual elements of the proposed EDM ring are given in Table 2 and Fig. 5. They are defined by the choice of deuteron momentum acceptable for efficient deuteron polarimetry (p_D = 1.0 GeV/c), the readily attainable magnitude of the electric field at the chosen 2 cm distance between electrodes (E_R = 12 MV/m), and the free space between lattice elements needed for the chosen number of polarimeters (4). In addition, the CW-CCW procedure to cancel the E_V-field effect requires that the periodic sequence of the fields, $\vec{E}(s)$, $\vec{B}(s)$, met by the particles moving clockwise be the same as the periodic sequence of the fields, $\vec{E}(-s)$, $-\vec{B}(-s)$, met by the particles moving counterclockwise. The $\vec{E}$-field is always directed outwards. The minimization of the second-order perturbations imitating the EDM requires that the magnetic field, B_V, of any bending magnet not be separated in space from the radial electric field, E_R, which we use for cancellation of the $g-2$ rotation in this magnetic field.

Table 2: **Deuteron EDM ring parameters**

Deuteron Momentum	1.0GeV/c
Rigidity, $(B-E/\beta)R$	3.336 Tm
Electric field, E_R, for $2a_x$ = 2cm	12MV/m (0.04 T)
Magnetic field, B_V	0.4819 T
Length of orbit, L	82.955m
$BE-$ section radius, R_0	8.4058 m
Length of the $BE-$ section, l_{BE}	3.3009 m
Number of regular periods, N	8
Horizontal tune, $\nu_x = \frac{f_x}{f_c}$	4.2520
Vertical tune, $\nu_y = \frac{f_y}{f_c}$	3.8019
Betatron amplitude functions, $(\beta_{x,y})_{\max}$	11.704 m; 13.256 m
Designed injected $\epsilon_{x,y} = \pi a_{x,y}^2/(\beta_{x,y})_{\max}$	3π mm mr; 10π mm mr
Momentum compaction factor, α	0.217
$(\Delta p/p)_{\max}$	10^{-3}
Quad gradient in bending section, B_q', for $l_g = 0.3$ m	370.6 Gauss/cm
Quad gradient in straight section, $l_g = 0.3837$ m	1174 Gauss/cm
Number of long straight sections, $N_{s.s.}$	2
Number of free intervals in one straight section	8

Inside the BE sections, $B = B_V$ is homogeneous, while $E = E_R = E_0\frac{R_0}{R} = \frac{E_0}{1+x/R_0}$, where R_0 = 8.406 m is the designed radius of curvature of the BE sections, E_0 is the

radial electric field at that radius, and $x = R - R_0$. Our design takes into account the corresponding small corrections of the betatron radial and synchrotron longitudinal frequencies caused by the radial electric field. In the beam dynamics, our long straight sections are represented by unit matrices for both radial and vertical oscillations. In such a design, our beam manipulations in the semicircles will minimally influence the beam parameters in the straight sections.

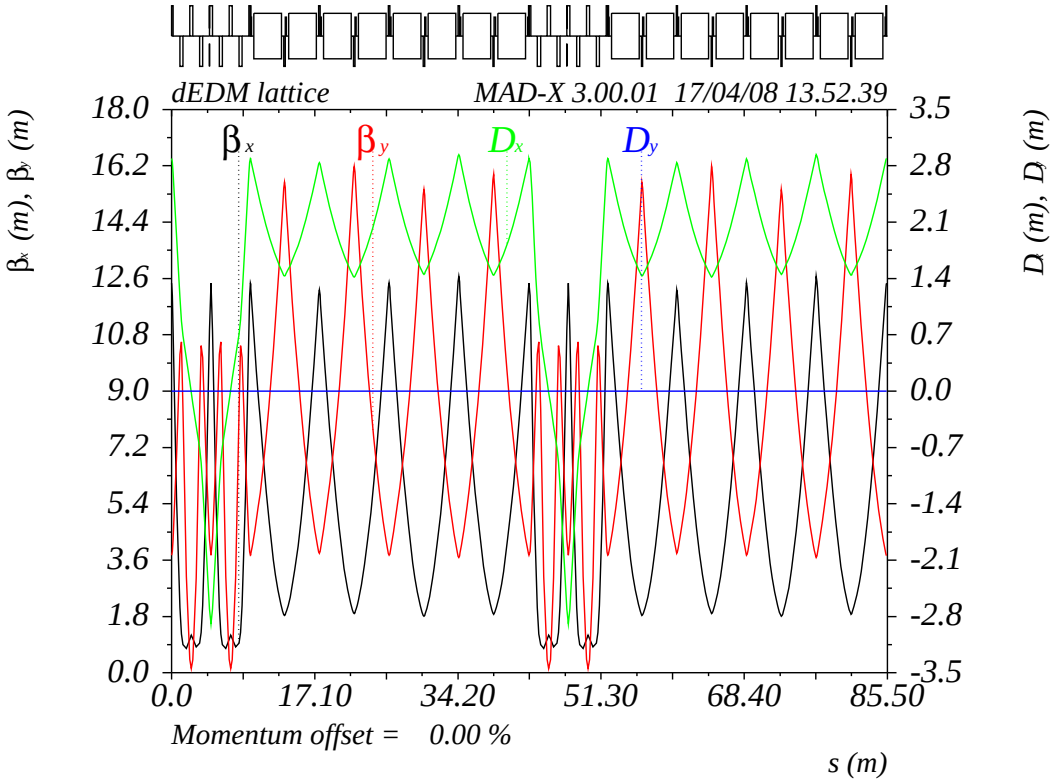

Figure 5: The deuteron EDM ring lattice. The parallelograms on the top of the figure depict the dipole magnetic field regions, while the thin vertical lines correspond to focusing and de-focusing magnetic quadrupoles. The red and black lines show the corresponding vertical and horizontal beta-functions as a function of the azimuthal position. The green and blue lines show the corresponding values for the horizontal and vertical D-functions as a function of the azimuthal position.

Special care is taken with respect to the accuracy of the same absolute value of the vertical magnetic field, $|B_V|$, in CW vs. CCW runs. If $\delta B_V = |B_V|_{CCW} - |B_V|_{CW} \neq 0$, then the equilibrium radius, and hence the trajectory length of the CCW particles, differ from those of the CW particles,

$$\frac{\delta L}{L} = \left\langle \frac{\delta R}{R} \right\rangle = -\alpha \frac{\delta B_V}{B_V} \neq 0. \tag{32}$$

$\alpha = 0.2166$ is the compaction factor from Table 2. Further, due to synchrotron stability, the revolution frequency, $f_c = \frac{\beta c}{L}$, is the same for CW and CCW particles. Therefore, a deviation $\frac{\delta L}{L} \neq 0$ leads to the corresponding deviation of the velocity,

$$\frac{\delta \beta}{\beta} = \frac{\delta L}{L} \neq 0. \tag{33}$$

This, in turn, leads to an error in the cancellation of the value of $\frac{E_V}{\beta\gamma^2}$ by the CW-CCW method,

$$\delta\left(\frac{E_V}{\beta\gamma^2}\right) \sim \alpha\left(\frac{E_V}{\beta\gamma^2}\right)\left(\frac{\delta B_V}{B_V}\right). \tag{34}$$

This error is easily controlled by our preliminary cancellations of the vertical electric field up to the needed level. The needed level will depend on our preliminary knowledge of the upper limit on the dEDM. If, for example, we already know that the dEDM $< 3\times10^{-25}\,\mathrm{e}\cdot\mathrm{cm}$ then, we will need to cancel the vertical electric field up to the level corresponding to that accuracy, which is $E_V/E_R \leq 10^{-10}$ in every fill. It is important to note that we will *not* measure E_V to that accuracy directly. Instead, we will measure E_V indirectly by observing the vertical component of the deuteron polarization during a single fill (lasted approximately 1000 s), and then correct E_V. After that, we will have the E_V-perturbation in our ring only at that level. Then one CW and one CCW run will cancel this perturbation, if $\delta B_V/B_V$ <150 ppm, which can be very easily achieved.

RF cavities are needed in our ring to increase the spin coherence lifetime, as explained in the next section. Deuterons are not accelerated, but an energy loss of about 0.05 eV per turn is expected if we use the gas in the beam path to extract the beam. This energy loss will be compensated for by the electric field in the RF-cavity. We have estimated that this effect requires the RF-cavity to be aligned with respect to the E-field plane at the 10^{-4} radian level, which is easily attainable.

4.2 Polarization Lifetime (Spin Coherence Time)

In our lattice design, the spin coherence time is near 1000 s. During this time,

$$\omega_a = \frac{e}{m}\left[aB_V - \left(a - \left(\frac{mc}{p}\right)^2\right)\beta E_R\right] \tag{35}$$

is controllably small, $\omega_a \sim 0.001\ \mathrm{s}^{-1}$. With such a small ω_a, we have no spin resonances at the betatron and synchrotron frequencies. Nevertheless, there exist effects depolarizing the beam. We can conclude directly from Eq. (35) that particles having different momenta have different g-2 frequencies. It is obvious also that the magnetic and electric fields met by particles depend on their betatron amplitudes. Moreover, a deeper analysis shows that the equilibrium momenta of particles with different betatron amplitudes are also different. Thus, the undesirable depolarization effects are mostly caused by the spread of the particles' betatron and synchrotron deviations. In a linear approximation, in the commonly used notation,

$$x(s) = \langle\Delta x\rangle + D(s)\frac{\Delta p}{p} + A_x\sqrt{\beta_x(s)}\cos\left(\psi_x(s)+\delta_x\right)\ \text{, horizontal} \tag{36}$$

$$y(s) = A_y\sqrt{\beta_y(s)}\cos\left(\psi_y(s)+\delta_y\right)\ \text{, vertical} \tag{37}$$

$$\frac{\Delta p}{p} = \langle\tfrac{\Delta p}{p}\rangle + \left(\frac{\Delta p}{p}\right)_{max}\cos\left(\omega_L t+\delta_s\right)\ \text{, momentum,} \tag{38}$$

where $\langle\Delta x\rangle$, $\langle\Delta p/p\rangle$ are shifts of the particle equilibrium due to the nonlinear effects explained below. $\langle ...\rangle$ means averaging over time, and $D(s)$ is the dispersion function. s is the longitudinal coordinate, and the synchrotron frequency ω_L is much smaller than the betatron frequencies, $\nu_L \ll \nu_{x,y} \equiv f_{x,y}/f_C$. If the Courant-Snyder betatron functions $\beta_{x,y}$ are given in meters, see Table 2, then the amplitudes $A_{x,y}$ are measured in $\mathrm{m}^{1/2}$, and when, say, $y_{max} \sim 1.0$cm, $A_y^2 \sim 10^{-5}$ m. Due to betatron and synchrotron oscillations, all

first-order (linear) spin perturbations related to the spread of $x,\ y$, and $\Delta p/p$ vanish on the average (in time) for every individual particle. Without the synchrotron RF, momenta would not oscillate ($\omega_L = 0$), and with the spread $|\frac{\Delta p}{p}| = 10^{-3}$, the beam would be depolarized after 1 ms.

With RF cancellation of the first-order contributions to the depolarization, we turn to second-order effects. In the second approximation, the shifts present in Eqs. (32, 34) are not equal to zero. This follows from the fact that, in the presence of synchrotron stability, the averaged (over time) revolution frequency is the same for all particles. Therefore, $\langle \Delta p/p \rangle$ is connected with $\langle \Delta L/L \rangle$, which, in turn, is connected with $\langle \Delta x \rangle$, $A^2_{x,y}$, and so on.

The quadratic effects of spin decoherence time and its extension in an electron-positron storage ring were investigated experimentally, and in part theoretically, in the Budker Institute [34, 35]. The results of our independent theoretical analysis are completely consistent with their experimental results, taking into account the difference between their electron-positron and our EDM deuteron storage rings. In our ring, if no special measures are taken, then the deviation $\Delta\omega_a$ of a particle having parameters $A_x,\ A_y,\ (\frac{\Delta p}{p})_{max}$, from the designed ω_a-value is given by

$$\frac{\Delta\omega_a}{e|a|\frac{B}{m}} \approx (0.65\,\mathrm{m}^{-1})A_x^2 + (0.16\,\mathrm{m}^{-1})A_y^2 + 0.84\left(\frac{\Delta p}{p}\right)^2_{max}, \tag{39}$$

$$\frac{e}{m}|a|B = 2\pi \times 275.51\,\mathrm{kHz}\,. \tag{40}$$

The spin coherence lasts nearly 1 s, when the maximal x in the beam equals 0.6 cm ($\epsilon_x = 3\pi$ mm-mrad), the maximal y equals 0.7 cm ($\epsilon_y = 5\pi$ mm-mrad), and $(\frac{\Delta p}{p})_{max}$=0.001, and synchrotron stability is present. We cancel these "natural" effects by counter-effects, using different sextupole lenses in the intervals between dipoles and a small quadratic field component inside dipoles. The cancellation accuracy 0.1% will guarantee the 1000 s spin coherence time. The magnitude of the sextupole (quadratic) $B^{''}$ fields will depend on their distribution along the ring. We plan to have $B^{''} \sim 1$ Tm^{-2} in the dipoles and not more than 20 Tm^{-2} in the lenses between dipoles.

The cancellation of the quadratic terms proceeds as follows. Consider some oscillator with a quadratic nonlinearity,

$$\frac{d^2z}{dt^2} + \omega^2 z = kz^2. \tag{41}$$

The equilibrium position of this oscillator has the non-zero value $z = \langle z \rangle = k\frac{\langle z^2 \rangle}{\omega^2}$, averaged over time. This fact lies at the basis of the idea of decoherence cancellation by quadratic fields. The vertical component of a sextupole field equals

$$\frac{1}{2}\frac{\partial^2 B_V}{\partial x^2}(x^2 - y^2). \tag{42}$$

Its horizontal component does not influence spin, on the average. The shift of the horizontal equilibrium, $\langle x \rangle \neq 0$, produced by such a field is proportional to

$$0.5B''\left(\langle x(s)^2\rangle - \langle y(s)^2\rangle\right) = 0.25B''(s)\left[\beta_x(s)A_x^2 - \beta_y(s)A_y^2 + D^2(s)\left(\frac{\Delta p}{p}\right)^2_{max}\right], \tag{43}$$

where all parameters are the same as in Eqs. (35)-(40). The equilibrium shift depends on a particle's parameters and changes the length L of the trajectory of this particle. Since the rotation frequency, $f_C = \beta c/L$, is fixed by the synchrotron stability, the particle momentum is changed. These shifts change ω_a. In our design, this $\Delta\omega_a$ is opposite to the "natural" $\Delta\omega_a$.

4.3 Non-Commutativity of Spin Rotations Imitating the EDM Rotation

At the very basis of a class of second-order effects imitating the EDM spin rotation lies the fact that rotations around different axes generally do not commute. If there is a set of consecutive rotations around different axes, that is, with different angular vectors, $\vec{\omega}_1 t_1$, $\vec{\omega}_2 t_2$, $\vec{\omega}_3 t_3$, $\vec{\omega}_4 t_4$, ..., and the sum $\Sigma \vec{\omega}_i t_i = 0$, (a closed loop), then the integrated spin rotation is *not* zero. In particular, if the closed loop of these vectors lies in a plane, then the spin is rotated around the axis perpendicular to this plane.

This is demonstrated in a simple and relevant example. Let $\delta_1 = \omega_a t_1 \ll 1$ be a small angle of rotation around the vertical axis due to a local deviation of ω_a from zero (due to, say, some level of the dipole magnetic field, ΔB_V, exceeding the designed value). Let $\delta_2 = \omega_L t_2 << 1$ be a small angle of rotation around the longitudinal axis due to some local longitudinal magnetic field, B_L. Last, let the rotations restoring zero sum be $\delta_3 = -\delta_1$, and $\delta_4 = -\delta_2$. From the linear equation for the spin, $d\vec{s}/dt = \vec{\omega} \times \vec{s}$, we can easily find the spin transition matrices for all four rotations, and their product M, keeping only up to second-order terms:

$$\begin{aligned} M &= \begin{bmatrix} \frac{1}{\sqrt{1+\delta_2^2}} & -\delta_2 & 0 \\ \delta_2 & \frac{1}{\sqrt{1+\delta_2^2}} & 0 \\ 0 & 0 & 1 \end{bmatrix} \times \begin{bmatrix} \frac{1}{\sqrt{1+\delta_1^2}} & 0 & -\delta_1 \\ 0 & 1 & 0 \\ \delta_1 & 0 & \frac{1}{\sqrt{1+\delta_1^2}} \end{bmatrix} \\ &\times \begin{bmatrix} \frac{1}{\sqrt{1+\delta_2^2}} & \delta_2 & 0 \\ -\delta_2 & \frac{1}{\sqrt{1+\delta_2^2}} & 0 \\ 0 & 0 & 1 \end{bmatrix} \times \begin{bmatrix} \frac{1}{\sqrt{1+\delta_1^2}} & 0 & \delta_1 \\ 0 & 1 & 0 \\ -\delta_1 & 0 & \frac{1}{\sqrt{1+\delta_1^2}} \end{bmatrix} = \begin{bmatrix} 1 & 0 & 0 \\ 0 & 1 & -\delta_1\delta_2 \\ 0 & \delta_1\delta_2 & 1 \end{bmatrix} \end{aligned} \tag{44}$$

We see that the result of two small rotations and counter-rotations around the vertical and longitudinal axes is a quadratically small rotation around the radial axis, the rotation precisely imitating the EDM.

An important detail of our ring design is that the E and B fields, which cancel each other in spin dynamics, are combined at the same locations, so δ_1, δ_2, ... are very small. If this were not done, some δ_1, δ_2, ... would be big and we would have additional first-order perturbations.

It should be added that many second-order systematics can be distinguished in data analysis from an EDM signal. Concrete examples of such errors (designated as δ_1, δ_2 in our analysis above) include (1) longitudinal magnetic fields from bending magnet misalignment in the presence of a finite $g-2$ rotation, (2) longitudinal magnetic fields mixed with locally high and low values of the bending magnet field even if $g-2$ rotation is cancelled on average, and (3) a non-vanishing local $\vec{E} \cdot \vec{B}$ in the presence of a finite $g-2$ precession. In this example, the size of the resulting vertical polarization is independent of ω_a, unlike the EDM signal which varies with ω_a as in Eq. (16). To the extent that the components of the error cycle are spread out around the ring, polarimeters in different locations will record different results, unlike the EDM signal which is the same everywhere.

In some cases, such as the error arising from $\vec{E} \cdot \vec{B} \neq 0$, the vertical Fourier component is $\cos\xi$ rather than $\sin\xi$. Thus, in addition to the CW $\leftrightarrow$ CCW method, and procedures minimizing the driving errors behind second-order effects, analysis signatures exist that can separate them from the EDM signal.

4.4 Magnetic/Electric Field: Monitoring and Feedback Stabilization

In order to cancel the deuteron $g-2$ precession with a relative accuracy of 10^{-9}, we need to control the *relative* values of the magnetic and electric fields at the same level. We will

do so in two ways: (1) by the deuteron $g-2$ (or horizontal) precession angle, and (2) by NMR techniques (magnetic field) and the Kerr effect (electric field).

(1) The statistical error in the determination of the horizontal spin precession angle is given by $\delta\omega_a = 2\sqrt{2}/(\tau\ it_{11} iT_{11}\ \sqrt{Nf})$, where τ is the beam lifetime, it_{11} and iT_{11} are the beam polarization and analyzing power, respectively, and f is the efficiency of the polarimeters. With a single store of 4×10^{11} polarized deuterons, it will be possible to determine the horizontal spin precession angle with a statistical error of the order of $10\,\mu$rad. Taking into account that π radians within a 10^3 s storage time would correspond to 10^{-9} relative stability between the B and E fields, it is obvious that the relative field knowledge from a single measurement will be of the order of 10^{-12}, much better than needed [1]. This knowledge will be used to control ω_a with feedback to trim magnets and E field electrodes to the desired level.

(2) The magnetic field can be measured and stabilized with a relative sensitivity of better than 10^{-8} every 50 s using NMR techniques. The electric field relative stability will also be monitored using the Kerr effect by monitoring the laser polarization state of a beam traversing a birefringent crystal in the electric field region.

5 Systematic Errors

5.1 Systematic Errors Due to Electric and Magnetic Field Imperfections

The dominant spin related systematic error ($< 10^{-29}\,\mathrm{e}\cdot\mathrm{cm}$) is due to $\langle E_V\rangle$, which we now discuss in detail. In a storage ring with only magnetic fields, a particle follows an orbit such that the average radial magnetic field is zero. Otherwise there is a net vertical Lorentz force, and the particle would not be stored. With an average vertical electric field $\langle E_V\rangle$, the storage requirement on the average vertical force is

$$\langle F_V\rangle = e(\beta c\langle B_R\rangle + \langle E_V\rangle) = 0. \tag{45}$$

This gives an average radial magnetic field in the particle's rest frame

$$\langle B_R^*\rangle = \gamma\left(\langle B_R\rangle - \beta\langle E_V\rangle/c\right) = \frac{\langle E_V\rangle}{c\beta\gamma}, \tag{46}$$

which precesses the spin about the radial direction:

$$\omega_{E_V} = \frac{ge\langle E_V\rangle}{2mc\beta\gamma^2}. \tag{47}$$

This is the only first order spin dynamics systematic error, i.e. this error by itself produces a systematic effect. The precession ω_{E_V}, relative to ω_{edm}, changes sign when we inject the beam clock-wise (CW) vs. counter-clockwise (CCW). The EDM signal is a difference in the measured deuteron spin precession about the radial direction when injecting CW vs. CCW. Without this symmetry, $E_V/E_0 < 5\times10^{-15}$ would be required for an EDM systematic error of $10^{-29}\,\mathrm{e}\cdot\mathrm{cm}$.

The CW/CCW procedure will not perfectly cancel the $\langle E_V\rangle$ systematic error because:

1. The CW/CCW runs are taken at different times separated by $\simeq 10^3$ s.

2. The spatial extent of the beam will be different CW/CCW.

[1] In reality the g-2 precision will be limited by the spread in frequencies due to horizontal and vertical betatron oscillations, which limit the SCT. The accuracy will be 10^{-9}, exactly at the needed level.

3. There may be systematic changes in E_V when the magnetic field is reversed during the CW/CCW procedure. Note that the electric field is not reversed during the CW/CCW procedure.

4. The magnetic field does not reverse perfectly CW/CCW.

We now discuss these in order.

1. Ground Motion and Temporal stability of $\langle E_V \rangle$

The average vertical E-field will also have a time-dependent component, which may not be compensated by the CW and CCW technique since they will be occurring at successive times. The physical effects responsible for the time varying component of the vertical E-field are 1) ground motion and 2) temperature effects.

1) In order to assess the magnitude of the first effect, we have tooken measurements of the floor movement near the intended EDM ring location. The AGS floor consists of a 3-ft thick floor interspersed with trenches. We have taken the data with two accelerometers located a) next to each other, b) 5 m apart, c) 10 m apart and d) 25 m apart, always keeping them on the same side of the trenches, i.e., keeping them on the same concrete block. Figure 6 shows the ground acceleration ($\mu m/s^2$) vs. frequency (Hz). Figure 7 shows the coherence between the two signals as a function of frequency. The low frequency motion is coherent, as expected. We plan to take coherence data down to mHz to confirm with measurements the common knowledge among the experts in the field that the very low frequency noise is coherent for a ring size of approximately 20 m by 20 m. Figure 8 shows the response spectrum of the AGS floor, indicating that any system mounted on it should have a resonance frequency outside the frequency range of 20-100Hz in order to avoid unwanted resonances. From Fig. 7 and above 1 Hz, which we will assume to be incoherent, we can determine that the floor moves vertically[2] by 100 nm. Assuming the motion to be random and incoherent (uncorrelated) at distances more than 1 m apart, the average motion over the 80 m circumference length would be about 10 nm. This average over 10^7 seconds would be 3.5×10^{-12} m. This small ground motion would still cause an effect about one order of magnitude higher than the sensitivity of the experiment for $10^{-29}\,\mathrm{e}\cdot\mathrm{cm}$. In order to eliminate the ground motion as a systematic error we have chosen to run two beams at the same time, CW and CCW tracing two rings on top of each other. The E-field plates are shown[3] in Fig. 9, and Fig. 1 shows the magnetic field design with two dipole magnetic fields of opposite polarity at 40 cm vertically. Clearly the design of the E-field plates (most importantly) and of the magnets (less importantly) needs to exhibit no resonances in the frequency range 20-100 Hz. Any ground motion, in the absence of resonances in the 20-100 Hz frequency ranges, will be effectively the same in both the top and bottom beam locations and will cancel.

2) Temperature effects are very important and special attention needs to be paid to them. The EDM ring will be placed on an existing 3-ft thick concrete floor. The ring itself will be covered on all sides by concrete blocks 4-ft thick as well, for radiation control issues. The concrete will create a thermal enclosure, which in the absence of any thermal sources inside the ring, will keep the temperature uniform and stable in time. The main thermal sources are the (normal) conducting magnets, each of which is estimated to require 5 MW of power (mainly due to the dipole magnets). Each coil temperature will rise by 10 K. This power will be taken out by cooling water flowing through the copper coils in

[2]Our data taken with sensor sensitive to horizontal motion indicate a similar spectrum

[3]When storing the beam CW and CCW, the electric field remains in the same direction whereas the magnetic field needs to be opposite in sign.

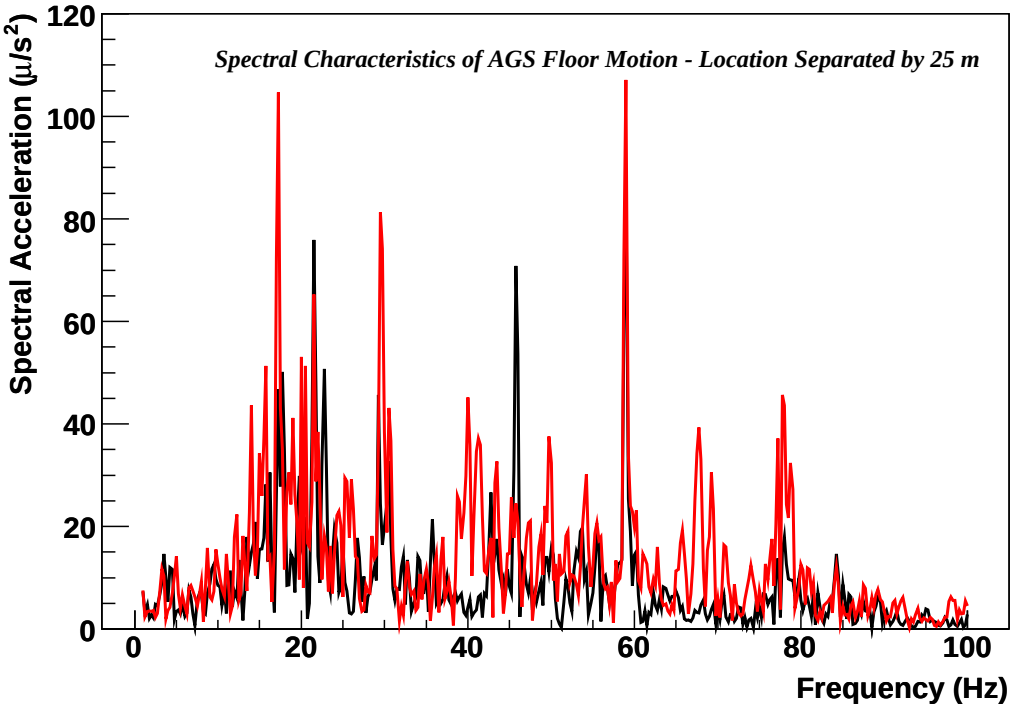

Figure 6: Acceleration data in μm/s^2 vs. frequency in Hz, taken at the AGS experimental floor with two probes separated by 25 m.

special channels. We plan to control the coil temperature to 0.1 K with a time constant of about 100 s. The power removal control will be made to $\pm 1\%$ per magnet, which means that there is going to be on average ± 10 KJ of energy released into the interior of the thermal enclosure every second. It is estimated that the total concrete volume will be 1500 m^3; taking into account that it requires 2 MJ to raise the concrete temperature by 1 K for every 1 m^3, it will take 100 s for the temperature to change by 3×10^{-4} K. For the duration of the experiment (10^7 s) the fluctuations are going to be, on average, at the level of 10^{-6}. The expansion coefficients of many materials are 10^{-5}/K, meaning that the average expansion over the experiment time is 10^{-11}. The induced angles over 25 m will also be 10^{-11} rad. This is indeed much higher than the strict requirements of the experiment. However, the main effect of tilting an electrostatic-plate is the creation of a vertical electric field common to both top and bottom rings, and therefore it will cancel. However, the higher-order components of the electric field will not cancel in both rings. We are planning to have a flatness per electrostatic plate (on average over the entire plate) of $\delta x = 1$ μm and keep the plates parallel to each other to the same accuracy. The quadrupole component of the field will be, on average, 1 ppm per plate at about 1 cm from the center. The field in each plate will be

$$E_y = \frac{V\theta}{2d}\left(1 + \frac{\delta x}{d}\right). \tag{48}$$

Clearly, the quadrupole component of the E-field does not pose any problem due to the temperature stability, as long as it is less than 100 ppm of the radial component at a radius of about 1 cm.

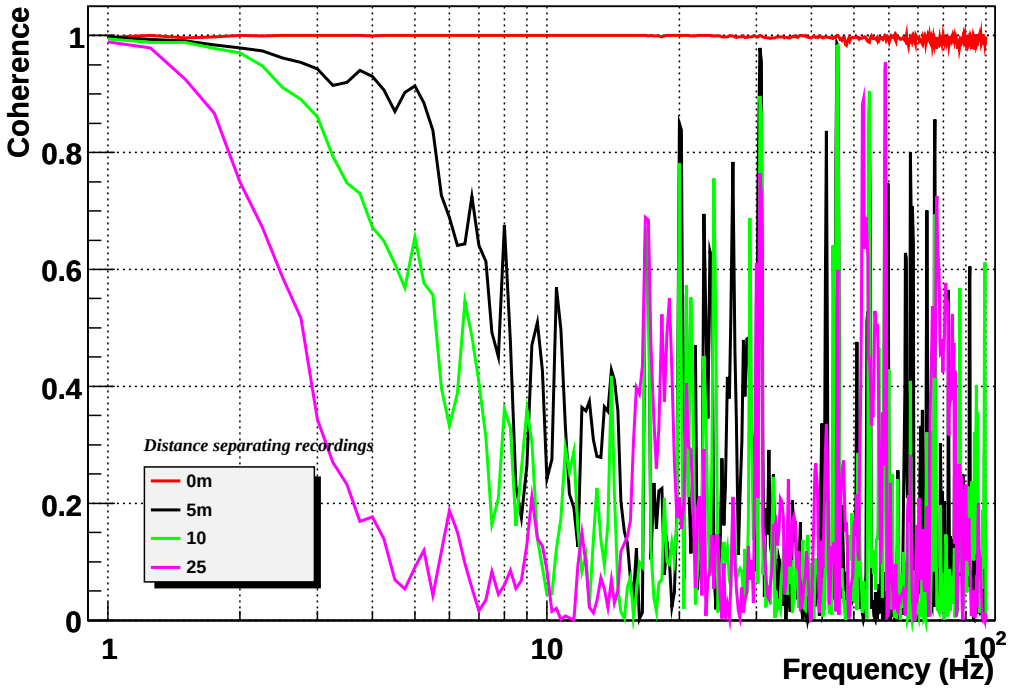

Figure 7: Coherence between various points of the AGS floor as a function of frequency for various distances between the probes.

2. Spatial reproducibility of the beam CW/CCW

In order for the CW and CCW injections to cancel the systematic errors, the injected beam distribution needs to be "exactly" the same for CW and CCW. How "exactly" the same depends on the multipole content of the vertical electric field.

Computer simulations of the field of realistic electrodes using the 2-D computer program OPERA [36] were performed. The design was guided by the desire to reduce the dipole component of $E_{\rm V}$ as well as higher-multipole components. The amplitudes of $E_{\rm V}$ compared to the radial E-field amplitude are all below (on average over all the plates) 0.2 ppm as is shown in Table 3.

Table 3: $E_{\rm V}$ **Multipole content at** $R = 0.9$ **cm from the center of the storage region normalized to the radial E-field.**

N	0	1	2	3	4	5
$E_{\rm V}(N)/E_{\rm radial}$ [ppm]	0.01	0.2	0.02	0.006	0.0002	0.0001

The quadrupole component ($N = 1$) is equal to 0.2 ppm, i.e. 2×10^{-7} at $R = 0.9$ cm. Since the CW and CCW contributions need to cancel at the 0.3 prad level, the beam needs to repeat the average radial beam position to 0.5 nm, which can be measured with pickup electrodes. However, we plan to measure the $E_{\rm V}$ quadrupole component by moving the beam to about 1 mm larger radius, and then apply a correction to a trim electrode. If we trim the field to 0.25%, the pickup electrode requirements will be much more relaxed. They would have to be able to measure the difference of the average beam position between

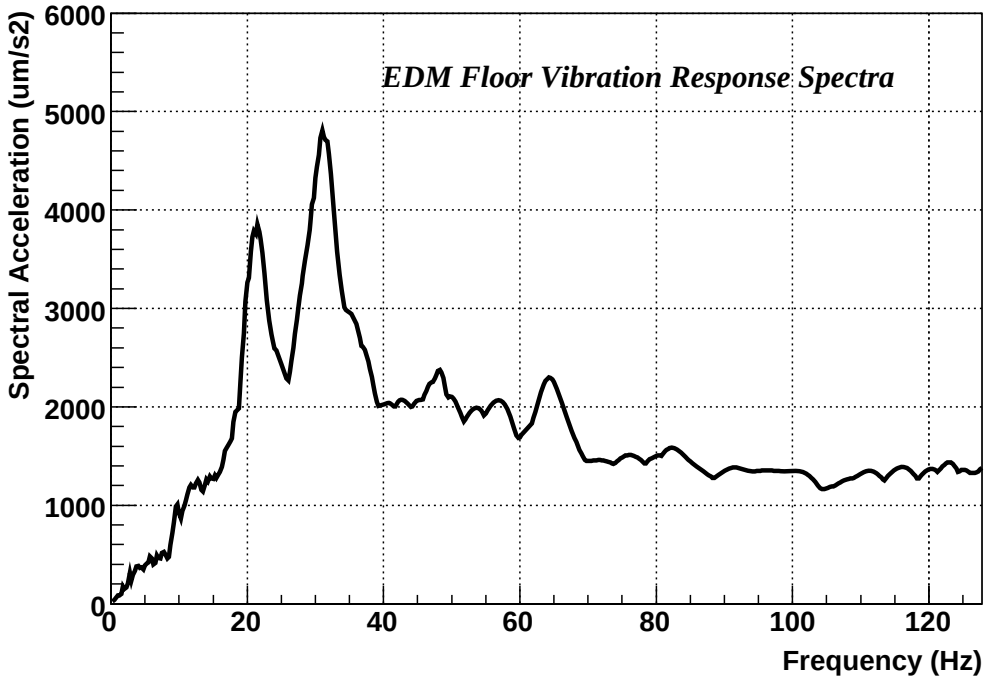

Figure 8: Response function of the AGS experimental floor as a function of frequency.

CW and CCW of about 1 μm, which is already done in many storage rings.

The sextupole and higher-order components of E_V couple to the same components of the beam and again need to be the same CW and CCW. The requirements for the pickup electrodes in these cases are more relaxed than the quadrupole component. We also plan to reduce this problem further by making the beam multipole content at least ten times larger [37], in order to obtain sensitivity to the multipole content of E_V. We then will minimize E_V with sextupole and other trim electrodes. Data-taking will be done with the beam multipole contents minimized. The pickup electrodes, described in a later section, will monitor the beam multipole components throughout the experiment.

3. Systematic changes in E_V when the magnetic field is reversed during the CW/CCW procedure

To minimize the mechanical influence of the magnetic field on the electrostatic plates (ESP) the latter will be mounted independently of the magnet. The forces from the eddy currents on the vacuum chamber have been estimated to have a negligible effect on its mechanical stability. Even though the estimated effect from the magnetic field on the ESP orientation is expected to be below the sensitivity of the deuteron experimental goal, it is nevertheless important to verify this with a measurement. For a 60 cm plate height, 0.5 frad corresponds to 0.5×10^{-15} m shift in ESP, which is well within the capabilities of Fabry-Perot resonators using LIGO [38] techniques. The sensitivity level achieved at LIGO is more than 10^3 times better than our requirement at the 1-10 Hz frequency range. The idea is to install one mirror of the Fabry-Perot resonator on each plate of the ESP and test whether the plates move when the magnetic field value and/or its direction changes. This will first be performed on a test setup using up to a 1.5 T magnetic field, greatly in

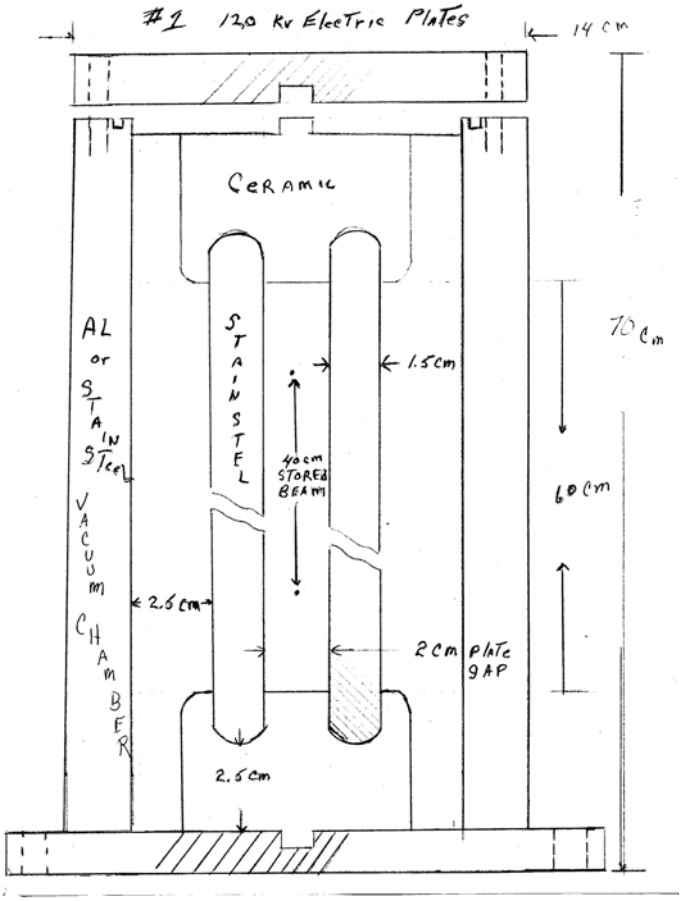

Figure 9: The electric field plates showing the beam locations 40 cm apart vertically traveling into and out of page. The electric field of one beam influencing the other beam is negligible due to shielding from the plates.

excess of the ≈ 0.5 T field required for the actual experiment with deuterons.

Our collaborators from Italy (Legnaro and Trieste) have developed a very sensitive, high finesse, Fabry-Perot resonator [39] for the needs of the PVLAS experiment using technology similar to LIGO. Their Fabry-Perot resonator, with the addition of a reference laser cavity, is expected to have the required sensitivity for our needs [40]. We expect this test to be the first we perform in the early stages of the experimental construction.

Another effect that could be different in going from CW to CCW is the so-called patch effect or floating charges. The materials in the vicinity of the storage region could charge up during the deuteron storage time, in which case the electric field would influence the stored beam. In order to avoid such a possibility, the materials would need to be made of conducting metal and grounded. Even so, a thin oxidized layer on their surface could develop with time. In the Berkeley Tl experiment, the electric field plates were originally made out of Aluminium [41]. An oxidized aluminum layer developed, which became a problem because it acted like a high voltage insulator accumulating charge [41]. This problem disappeared when they used Cu plates. The oxidized layer in Cu is conducting.

In our experiment we intend to pay special attention to minimizing the patch effect. Special care will be paid to avoid backstreaming into the vacuum system from the vacuum pumps. Finally, the electrical charges accumulated due to a non-conducting layer will be

mostly the same with CW and CCW injection.

4. Imperfect CW/CCW reversal of Magnetic Field

The presence of an EDM will cause the spin to develop a vertical component, i.e., the total spin precession plane will be out of the horizontal plane. As can be seen from Eq. (16) the influence of the EDM on the spin precession plane will be minimal when ω_a is not minimized, while the contrary is true when ω_a is minimized. Therefore, the EDM signal is the change of the spin precession plane between the following two running conditions: (1) the $g-2$ precession rate is minimized so that the deuteron spin is allowed to precess by about π rad within the 10^3 s storage period, and (2) the deuteron spin is allowed to precess 10π rad in a 10^3 s period. In order to be able to descern the EDM effect, the B-field direction between the above two conditions cannot be allowed to change more than that expected from the EDM effect itself.

With a 10^9 reduction of the $g-2$ precession, the ω_a rate will be of the order of 1 mrad/s, i.e. 1 rad in 10^3 s. For a 10^{-29} e$\cdot$cm deuteron EDM, the spin precession rate ω_{edm} will be of the order of 10 nrad/s or 10 μrad in 10^3 s, i.e. the EDM at the 10^{-29} e$\cdot$cm level causes the spin precession plane to tilt by a little over 10 μrad.

However, the definition of "horizontal" might be subject to detector alignment and acceptance considerations. In order to define this plane uniquely for each polarimeter, we will adjust the magnetic field, B, to cancel the $g-2$ precession at the 3×10^{-9} level. This allows the spin to make about five complete turns "horizontally". The tilt due to the EDM in this case is going to be small, less than 0.1 μrad, as is apparent from Eq. (16). Then to go to the 10^{-9} cancellation level, we only need to change the amplitude of the magnetic field by about $\Delta B/B = 3$ ppm. We can apply this extra magnetic field in the same direction as B to much better than 1 mrad, so that the total B-field orientation will change less than 3 nrad, a much smaller change than the 10 μrad expected from the EDM effect.

In every CW injection we will have up to three runs, with variable control of the $g-2$ precession rate, so that at the end of the three 10^3 s running periods the spin will make about 5, 2 and 1/2 horizontal turns, respectively. The differences of the spin precession plane for those running conditions will be uniquely determined for this CW injection. At the end of the above three runs we will go into CCW injection, repeating the same running pattern. At the end of this operation we will compare the two sets of results. In simple terms, the sum corresponds to a background effect while the difference corresponds to a genuine EDM signal.

5.2 Polarimeter Systematic Errors

The vector left-right asymmetry that carries the EDM signal will be small in comparison to a number of other signals recorded by the EDM ring polarimeters. In order to separate this component from these other asymmetries, including systematic sources of a $\sin\xi$ term ($\xi = 0$ along the momentum direction), the measurement plan requires allowing some residual anomalous precession ($\omega_a \neq 0$) and a continuous measurement of the beam polarization during the store. With full azimuthal coverage, the polarimeters will also measure down-up asymmetries, a comparison of left and right with down and up that is sensitive to t_{22} polarization, and changes at large scattering angle in the azimuthally averaged rate that is sensitive to t_{20} polarization.

With this information, we can define a set of requirements that must be met by any real EDM signal. These include:

- the correct phase dependence on ω_a.
- no dependence on $2\omega_a$.
- changing sign with the reversal of the vector polarization.
- reversal of the EDM effect when ω_a changes sign.
- magnitude of the EDM effect going as $1/\omega_a$.
- EDM effect not depending on location of the polarimeter.
- reversal when the beam direction changes between CW and CCW.

Such requirements provide a way to distinguish any true EDM signal from a number of other effects that create significant contributions to the left-right asymmetry. In all cases, there are multiple ways that various errors are easily distinguishable because they fail to meet the requirements listed above. The following errors are addressed:

- Any residual vertical polarization that remains after the preparation of the beam and the filling of the storage ring will remain constant throughout the store, since such polarizations are stable regardless of the sign or size of ω_a.
- Tensor polarization in the beam will create a left-right asymmetry whenever the polarization is not perfectly aligned with either the beam velocity or the magnetic field bending radius. Such asymmetries will oscillate with ω_a at double the precession frequency and will be independent of the magnitude of ω_a or the direction of the beam.
- Software separation of the vertical and horizontal asymmetries may allow some of the $g-2$ asymmetry to appear in the left-right data, but it will not change sign with the ω_a sign change nor increase in size as ω_a get smaller.
- False asymmetries due to improper alignment of the beam in the polarimeter will track none of the characteristics of an EDM signal.
- False asymmetries can arise due to saturation of the detector response at high rates that are themselves polarization-dependent. Such effects do not change with the sign and magnitude of ω_a in the proper way.
- No symmetry prevents the beam from acquiring a t_{20} polarization as it passes through the residual gas in the ring. As the store progresses, this induced polarization rotates with ω_a and generates a left-right asymmetry to the extent that it resembles a t_{21} polarization. Such effects again oscillate at double the precession rate. They are also indifferent to the sign of the beam polarization from the ion source and do not change sign when the direction of the beam reverses.

If ω_a is stable during the store, one analytic approach would be to fit the asymmetries using a Fourier series based on $\xi = \omega_a t$ and extract the coefficient of the $\sin\xi$ term associated with an EDM. This coefficient would then have to have the right properties when certain experimental parameters are changed (spin-flip, sign of ω_a, beam revolution direction) as well as varying with ω_a as $\omega_{edm}/\sqrt{\omega_{edm}^2+\omega_a^2}$.

To summarize how the EDM signal can be separated from other sources of a left-right asymmetry, the table (4) below lists the 6 causes of an asymmetry given above and testable characteristics for each cause. A plus indicates that for this test the asymmetry appears

to be the same as an EDM signal, and a minus indicates where there is a distinguishable difference. The tests include "term," determining which term in the Fourier series would carry information on this error; "spin-flip," the response to reversing the direction of the beam polarization; "sign ω_a," changing the direction of the anomalous precession; "mag. ω_a," measuring at more than one value of ω_a to learn whether the coefficient of the $\sin\theta_a$ term varies as $\omega_{edm}/\sqrt{\omega_{edm}^2+\omega_a^2}$ in Eq. (16); "locat.," comparing results from more than one place in the ring; and "CW/CCW" notes the response to changing the direction of the beam in the ring. Lastly, an estimate is provided of the level at which the cancellation or the removal of this cause might be expected to fail. The only error that appears to be potentially significant concerns changes during the store to the position or angle of the beam on target. After the table, individual causes for left-right asymmetries are discussed in more detail.

Here, items whose distinguishability depends on experimental conditions (marked with an asterisk) are explained.

Table 4: **This table lists a number of causes of an asymmetry and testable characteristics for each cause. A plus indicates that this cause appears to be the same as an EDM and a minus indicates where there is a distinguishable difference (see text for description of the asymmetries and characteristics).**

ERROR	term	spin-flip	sign ω_a	mag. ω_a	locat.	CW/CCW	sens. ($\mathrm{e}\cdot\mathrm{cm}$)
(1) source p_y	$-$	$+$	$-$	$-$	$+$	$-$	$< 10^{-29}$
(2) source t_{21}	$-$	$*$	$+$	$-$	$+$	$-$	$< 10^{-29}$
(3) det. rotation	$+$	$+$	$-$	$-$	$*$	$+$	$< 10^{-29}$
(4) off axis/angle	$-$	$-$	$-$	$-$	$*$	$-$	see text
(5) non-linear det.	$+$	$+$	$-$	$-$	$*$	$+$	$< 10^{-29}$
(6) self-polarization	$-$	$-$	$+$	$+$	$+$	$-$	$< 10^{-29}$

(1) A vertical polarization that is present when the beam is injected into the ring is constant independent of ω_a.

(2) Small tensor polarizations at the level of a few percent are expected from the ion source. With the polarization axis in the ring plane, a t_{21} tensor component generates a left-right asymmetry. The analyzing power $\langle T_{21}\rangle \sim 0.03$ is small because it is independent of the deuteron-nucleus spin-orbit force. But with p_{ZZ} only 0.02, the left-right asymmetry can be 4×10^{-4}, almost two orders of magnitude above our limit on an EDM signal. A larger tensor polarization could make this term more than an order of magnitude larger. This term is eliminated in the Fourier analysis where it appears with half the period of the EDM signal. The response to spin-flip depends on the manner of generating the spin reversal. If the direction of the spin axis is changed at the ion source, the different hyperfine RF transition units used will introduce a different and unrelated tensor contamination of the beam.

(3) An error that could generate a "$\sin\xi$" Fourier coefficient would be any "rotation" of the detector boundaries that separate the down-up system from the left-right system. Since this effect is tied to the direction of the horizontal polarization component, it remains the same in the Fourier series analysis when ω_a is reversed, unlike to the EDM signal that changes sign. Additionally, this error is independent of the size of ω_a and may be different for different polarimeters in the ring.

(4) Left-right asymmetries can easily arise in polarimeters from small misalignments of the position or direction of the beam from the nominal center line through the polarimeter,

or from some asymmetry in the efficiency of the detectors on opposite sides, including their associated electronics and data acquisition logic. This commonplace error has typically been cancelled for many experiments by flipping the sign of the polarization of the beam, since these asymmetries do not depend on such changes. The analysis can be made more robust by considering "cross-ratios" that involve both left and right rates and both spin states [42]. If the left-right asymmetry is small (which it is), then corrections to the cross-ratio that depend on the derivatives of the analyzing power with angle appear at third order because ϵ becomes a small parameter.

(5) Rates in the detectors are high, and photomultipliers as well as other systems are well-known to have gains that depend on rate. These effects result in a detector response that, while it may depend linearly on rate over some operating range, is no longer proportional to rate. The rate in our system is an oscillation (on top of a constant or falling background) that comes from the spin precession. The largest effect is the down-up asymmetry that originates from the radial component of the deuteron spin, even if the detector is close to the plane of the storage ring. So long as the rate-dependent changes are in a linear range, only the magnitude of the asymmetry is affected. If the response contains a quadratic term and is different on the left and right sides, then this feeds into the $\sin\xi$ term in the Fourier analysis. As the stored beam loses intensity, the size of this term changes. Its dependence on ω_a will distinguish it from an EDM signal.

(6) Self-polarization of the beam is possible [43] since the ratio of the forward-nuclear to the forward-Coulomb amplitudes may have a significant magnitude when integrated over the acceptance of the storage ring. This effect has not been observed with corroboration and might appear for the first time in this experiment. Scattering spin-one deuterons from residual gas may introduce a t_{20} moment that "smears" into a t_{21} polarization (and a left-right asymmetry) as the spin precesses in-plane. This is the only systematic error that gets larger as ω_a gets smaller. It is distinguished by its Fourier signature and the fact that it is independent of the beam polarization. An important ancillary signature is a steadily rising t_{20} and t_{22} polarization.

All of these systematic effects that appear in the operation of the polarimeter, including those such as t_{21} and self-polarization that are unique to spin-one beams, are distinguishable from an EDM signal in at least two ways. It will be important that the analysis consider and model any effects that appear in the experiment at a measurable level. Otherwise, poor reproduction of the data will generate noise in the coefficient of the EDM term that will limit the sensitivity of the experiment.

5.3 Pickup Electrodes

The beam itself is the optimal tool for understanding the operational characteristics of the EDM storage ring, and this tool is made available with a system of Beam Position Monitors (BPM). A BPM system is an integral part of all storage rings. The BPM system is primarily used to determine orbit properties, but it can also allow the measurement of the beta-functions, the dispersion and the bunch length. The EDM storage ring will require beam position monitors in both the arcs and in the straight sections. The monitors are needed in the arcs to sense differences in the radial position of the beam for CW and CCW injection. A difference in the radial position between CW and CCW injection leads to a difference in average velocities, which, in turn, affects the accuracy of the cancellation of the vertical electric field. Since the required cancellation is 0.1 ppm and the bending radius is about 8.5 m, the *relative* beam position must be measured to the order of 1 μm. The monitors are needed in the straight sections to sense changes in the beam position with respect to the polarimeters. Beam movement with respect to the polarimeter causes a false asymmetry. Since the expected asymmetry is 5×10^{-6}, the *relative* beam position here

must also be measured to the order of 1 μm. The number and position of the monitors will be better understood after measurements of field reversal accuracy on dipole and quadrupole prototypes have been made.

Beam position sensitivities of the order of 1μm have been achieved with pick-up electrodes. The typical configuration has two pairs of opposing conducting strips offset by 90°. Each strip subtends the same azimuthal angle. The electric and magnetic fields of the circulating beam induce currents in the strips. The strips may be capacitively coupled to the beam line, in which case the BPM is an electrostatic device, or the strips may form with the beam pipe a transmission line with well-defined impedance. While the fundamental limitation of these devices is the thermal noise power, the low signal levels (typically ~ 10 μV for ~ 1 mA of beam) require careful exclusion of the electromagnetic interference that is endemic to the accelerator environment.

6 Cooled deuteron beam

For the present parameters of the EDM ring, it is desirable to have a small horizontal beam size at the location of the plates. For maximum dispersion $D_x = 2.9$ m, rms momentum spread of 2.5×10^{-4}, maximum horizontal beta function of $\beta_h = 12$ m, and emittance of 3π mm mrad (95%, normalized), the total 95% beam radius in the horizontal direction is 10 mm, which barely fits into the 20 mm space between the plates.

After the EBIS injector upgrade, it is expected to have an rms momentum spread of the deuteron bunch of about 2.5×10^{-4}. The expected emittance for 10^{11} particles per bunch is about 5π mm mrad (95%, normalized). Such expected beam parameters almost satisfy the requirement for the EDM experiment and correspond to a full horizontal beam size of 26 mm at the plates.

However, the current momentum spread in the AGS is determined not by the injector but rather by the Booster. For example, the current momentum spread in the Tandem is very small (less than 10^{-4}), but in the AGS is about 5×10^{-4} rms. It seems to be determined by the process of adiabatic capture in the Booster. As a result, one may expect to have slightly larger values of the rms momentum spread at the AGS injection of about 5×10^{-4} rms.

If one wants to have a smaller emittance or if the momentum spread at the AGS injection happen to be bigger than expected, then electron cooling can be used to get small momentum spread. For example, with 95% normalized emittance of 1.6π mm mrad (3π mm mrad unnormalized) and an rms momentum spread of 2.4×10^{-4}, the full horizontal beam size in the location of the plates is 15 mm, which fits comfortably in the present design with 20 mm space. Such parameters will require a factor of 3 cooling in transverse emittance and maybe a factor of 2 in longitudinal cooling, based on expected beam parameters. Such modest cooling is easily achievable with a standard electron cooler. Note that electron cooling can provide much stronger cooling (for example, for momentum spread), which maybe needed to obtain a long spin coherence time.

To cool deuterons at the EDM energy requires a low-energy cooler (about 60 keV electron kinetic energy). Such a cooler is a common device. It can be built on the scale of 2-3 years by the Novosibirsk group (BINP). The total cost of such a cooler is about 1M Euros.

If installed in the AGS, the cooler needs to fit into the available space between the magnets. Such a cooling system was considered for the scenario of cooling a coasting beam, as well as a bunched beam, in the AGS. The required beam parameters were found to be achievable with cooling. However, cooling in the AGS is limited to just modest cooling due to the space-charge limit.

The safest way of getting a small momentum spread and emittance for the experiment is to provide cooling directly in the EDM ring, rather than in the AGS. This removes the problem of space charge and instabilities in AGS for a cooled beam. It allows one to get a very small emittance and momentum spread at the beginning of the experiment. The full space needed for such a cooler is 2.5-3 meters.

Electron coolers at low energies are well established devices which have been built for the last 30 years [44]. There are presently tens of electron coolers operating around the world. The most recent were built for 1) IMP (Lanzhou, China); 2) LEIR (CERN); 3) S-LSR (Kyoto, Japan). Coolers for Lanzhou and CERN were built by BINP, Novosibirsk, Russia.

7 DAQ and Electronics

In a precision experiment such as this, high demands are placed on the electronics and data acquisition. It must be able to handle very large amounts of data, and should not introduce systematic effects, such as those due to, *e.g.*, variations in the readout rate (deadtime) or other electronics or software related phenomena (buffering). Data flows from several quite different systems (polarimeter, tilt-meters, beam-position monitors, pickup electrodes, Fabry-Perot, PbO) must be dealt with seamlessly for reconstruction of the EDM signal. We will evaluate existing and proven data acquisition software, such as the Midas system (https://midas.psi.ch/), for use in our experiment.

The main source of data will be the polarimeters. Several configurations are being considered. At a minimum, the polarimeter readout system must be able to distinguish from which bunch (of the couple circulating in the ring) an event originates, either by implementing bunch-indexing or by allowing time reconstruction. More sophisticated capabilities, such as signal magnitude reconstruction (*e.g.* for particle identification) or vertex reconstruction require additional functionality.

Typically, polarimeter readout is based on recording the number of hits in each of its segments during several ms or longer. To track individual bunches circulating in the ring, a *set* of several scaler modules, each with a gate synchronized with the passage of a single bunch, would be sufficient. With Struck Innovative Systems (http://www.struck.de/), implementation of this functionality in their SIS3820 multi-purpose scaler has been studied. It is expected that up to 40 individual 32-channel scalers with up to 50 MHz cycling can be implemented. For our application, this might be sufficient, resulting in a robust, extremely compact and undemanding setup.

The polarimeter will detect several percent of the of deuterons extracted from the ring. Over the course of a fill, this will amount to 10^{9-10} events, or 10^{6-7} events per second. Readout of such an event rate using multi-hit time-to-digital converters (MTDCs) can be accomplished with presently available electronics, *e.g.*, the CAEN V1290 MTDC. The corresponding data volume will amount to $4-40$ MB/s, well within network or disk throughput limits. A DAQ system based on this scheme is being prepared for use during the upcoming experiments at COSY-Jülich, where its performance and suitability for polarimetery will be tested. At the same time, the KVI-developed DAQ software package Caddie will be tested.

If, besides the arrival time, the magnitude of the signal also needs to be measured, readout using sampling ADCs (waveform digitizers, WFDs) is the best choice. At a typical event size of 100 bytes per event, the primary data stream will increase significantly (0.1–1 GB/s). On-line pulse-shape analysis using FPGAs (field-programmable gate arrays) built into the WFD modules, or via in-crate analysis computers is expected to reduce the stored data volume to about twice the data volume of the MTDC-only scheme.

A polarimeter based on the micro-megas-TPC or MRPC allows particle identification, and in the case of the TPC also reconstruction of the scattering vertex. Both systems consist of a detector placed close to the scattering target, resulting in increased rates. These systems place correspondingly heavy demands on the readout system.

Here we state the case for the micro-megas, but a similar system would be required for the MRPC. The maximum rate expected in the micro-megas-TPC detector is 5×10^7/s. For 10 cm drift space, a track requires about 2.3 μs to reach the readout plane. Thus, a maximum of 92 tracks at all times should be able to be handled by the system. The readout electronics could be similar to the T2K electronics for their micro-megas-TPC. It consists of preamplifiers and 40 MHz WFDs to sample the pad signals. Our design requires 3284 to 4612 readout channels. The cost per electronics channel is of the order of 10 Euros. The total cost of these will be about 46 kEuros. A rough estimate of the cost of the data acquisition and triggering system is about 50 kEuros. Thus the electronics and readout system cost is estimated to be 100 kEuros for the micro-megas-TPC.

8 Cost and Schedule

After the proposal is approved, we expect to complete a Technical Design Report (TDR) in roughly six months. After a successful review of the TDR, we will work on the proof of principle of the Fabry-Perot resonator to achieve the required level of accuracy. In parallel, we will develop the design of the E-field plates and demonstrate the proof of principle by operating them at full voltage in the required magnetic field. With the Fabry-Perot resonator, we will have to show that reversing the B-field does not influence mechanically the E-field plates at the required level.

At the same time, we will further develop spin and particle tracking programs to guide the design of the deuteron EDM storage ring. We expect to be ready to start the ring construction three years after the approval of the proposal. The ring construction will take two years to complete, at which point we will be ready to take beam. In the first year, we will have an engineering run to shim the B and E-fields and to achieve the required deuteron spin coherence time. During the second year, we will be ready for a physics run. We thus expect to have taken the required data by the end of 2013.

The estimated construction costs for the proposed experiment to search for the EDM of the deuteron in a storage ring at BNL are given in the following sections [4].

8.1 Storage Ring

16 dipole magnets @ \$50 K each		800 K
48 quadrupole magnets @ \$25 K each		800 K
32 sextupole magnets @ \$15 K each		480 K
Dipole power supply		250 K
Quadrupole magnet power supply		250 K
RF cavity & associated equipment		150 K
Vacuum & vacuum instrumentation		750 K
16 electric field regions with power supplies		1,000 K
Controls		160 K
Beam instrumentation		350 K
20 m diameter storage ring shielding		1,000 K
	Sub-Total	**\$5,990 K**
	Including Burdens	**\$17,670 K**
Injection kicker magnet & PFN		2,123 K
	Sub-Total	**\$19,793 K**

8.2 Experimental Systems

Tiltmeters		100 K
Fabry-Perot interferometers		300 K
NMR and Kerr effect system		300 K
4 Polarimeters, including data acquisition system.		929 K
Electron cooling		1,650 K
	Sub-Total	**\$3,229 K**

8.3 Total deuteron EDM ring cost

	\$23,022 K

8.4 Beamline and Conventional Facilities

In addition to the ring-experiment cost, the total cost of a beamline from the AGS to the deuteron EDM ring is estimated (including full burdens) to be \$7M, bringing the total experiment cost to **\$30,022K** .

As noted, this cost estimate was prepared for building the deuteron EDM storage ring at BNL. Other sites, such as CERN, FNAL, and J-PARC are under consideration. Cost estimates will likely differ because of differences in the overhead rates, the amount of existing equipment and infrastructure that can be made available, and operating costs.

[4] Burdens include: Costs for labor (75%), EDIA (Engineering, Design, Installation and Assembly) (15%), contingency (25%) and additional charges (17%). Total costs for items without the indication "Including Burdens" were based on estimates from known costs, including burdens based on recent experience with sufficiently similar devices.

9 Conclusion

We propose a search for a deuteron EDM at the $10^{-29}\,\mathrm{e}\cdot\mathrm{cm}$ level. At this level, we will be sensitive to a non-zero deuteron EDM value predicted by a number of theories beyond the SM. The strength of the proposed method resides in the following features:

- The $g-2$ precession can be reduced to the required 10^{-9} level.
- Our storage ring design makes possible spin coherence times greater than 10^3 s.
- High intensity (4×10^{11} per cycle), highly polarized deuteron beams are readily available.
- Polarimeters with high analyzing power (0.5) are available in the energy range of interest.
- Potential systematic errors can be corrected by polarization measurements of counter-rotating stored beams and polarization reversals.

The successful conclusion of this experiment will constitute a major advancement in the quest for a non-zero EDM of a fundamental particle.

We are greatly indebted to Sidney Orlov for improving the style and readability of this proposal.

References

[1] J.H. Smith, E.M. Purcel, and N.F. Ramsey, Phys. Rev. **108**, 120 (1957).

[2] F.J.M. Farley *et al.*, Phys. Rev. Lett. **93**, 052001 (2004); hep-ex/0307006.

[3] Y.F. Orlov *et al.*, Phys. Rev. Lett. **96**, 214802 (2006); hep-ex/0605022.

[4] The application of spin dressing to the EDM search was independently suggested by D. Beck and D. Kawall. A semi-realistic case was studied and showed that the method is very promissing but many years away from complete development. Y.K. Semertzidis, EDM internal report on spin re-winding, 2007.

[5] "Deuteron EDM Proposal: Search for a Permanent Deuteron Electric Dipole Moment at the $10^{-27}\,\mathrm{e}\cdot\mathrm{cm}$ Level", M. Aoki *et al.*, proposal to the BNL AGS, September 2004. The document is available from our official web site: "http://www.bnl.gov/edm/".

[6] R. Gupta, *et al.*, "React & Wind Nb_3Sn Common Coil Dipole", Presented at ASC 2006, IEEE Trans. on Appl. Supercond., Vol. 17, No. 2, pp. 11301135 (2007); R.C. Gupta, "A Common Coil Design for High Field 2-in-1 Accelerator Magnets", Particle Accelerator Conference, pp 3345-3347 (1997).

[7] V.S. Kashikhin, *et al.*, "Development and Test of Single-Layer Common Coil Dipole Wound with Reacted Nb_3Sn Cable", IEEE Trans. on Appl. Supercond., Vol. 14, Issue 2, pp. 353356 (2004).

[8] L. Chiesa, *et al.*, "Magnetic Field Measurements of the Nb_3Sn Common Coil Dipole RD3c", Particle Accelerator Conference, pp 170-172 (2003).

[9] Normal conducting RF-cavities achieve much higher electric fields when their surfaces are treated with high pressure water rinsing (HPR). The same is true for Ti surfaces used as photocathodes in electron machines: B.M. Dunham *et al.*, Proceed. of PAC07, 1224 (2007), Albuquerque, New Mexico, USA.

[10] Lawrence Cranberg, Journal of Applied Physics **23**, 518 (1952).

[11] O. Prokopiev presentations on the FNAL electrostatic separators conditioning, available from
http://beamdocs.fnal.gov/DocDB/0023/002358/001/separator20
_hand_polish_jul21_2006.ppt,
http://www-btev.fnal.gov/DocDB/0029/002944/001/BTeV_EBS_Polsw
_Pwrsup.ppt, and
http://www.cap.bnl.gov/mumu/conf/collider-071203/talks/RJohnson2-071203.pdf.

[12] A. V. Akindinov, *et al.,* Nucl. Instr. & Methods A **532**, 611 (2004)

[13] The micro-megas detector, first published in I. Giomataris *et al.*, NIM **376** (1996) 29; it can work at very high rates since space charge effects are suppressed and has been used on COMPASS and NA48 experiments at CERN. The mm-TPC version is being developed for the T2K experiment in Japan and for the ATLAS inner tracker being developed at BNL.

[14] C.A. Baker *et al.*, Phys. Rev. Lett. **97**, 131801 (2006).

[15] B.C. Regan *et al.,* Phys. Rev. Lett. **88**, 071805 (2002).

[16] A.D. Sakharov, JETP Lett., **5**, 24 (1967).

[17] M.V. Romalis *et al.,* Phys. Rev. Lett. **86**, 2505 (2001).

[18] V.F. Dmitriev and R.A. Sen'kov, Phys. Rev. Lett. **91**, 212303 (2003).

[19] C.P. Liu and R.G.E. Timmermans, Phys. Rev. C **70**, 055501 (2004).

[20] I.B. Khriplovich, R.A. Korkin, Nucl. Phys. A **665**, 365 (2000), nucl-th/9904081.

[21] O. Lebedev *et al.*, Phys. Rev. D **70**, 016003 (2004).

[22] M. Pospelov and A. Ritz, Ann. Phys. **318**, 119 (2005), hep-ph/0504231.

[23] R.L. Garwin and L. Lederman, Nuovo Cimento **11**, 776 (1959).

[24] J. Bailey *et al.,* J. Phys. **G4**, 345 (1978).

[25] D.F. Nelson, A.A. Schupp, R.W. Pidd, and H.R. Crane, Phys. Rev. Lett. **2**, 492 (1959).

[26] N.F. Ramsey, Annu. Rev. Nucl. Part. Sci. 1990. 40:1-14.

[27] J.D. Jackson, *Classical Electrodynamics* John Wiley and Sons, Inc., 1974.

[28] A. Silenko *et al.*, January 9, 2003. It can be found at "http://www-ps.kek.jp/jhf-np/LOIlist/pdf/L22.pdf" and from our own web site "http://www.bnl.gov/edm/". J-PARC: Japan Proton Accelerator Research Complex, "http://j-parc.jp".

[29] Y. Satou *et al.*, Phys. Lett. B **549**, 307 (2002).

[30] V.P. Ladygin *et al.*, Nucl. Instrum. Mathods A **404**, 129 (1998).

[31] B. Bonin *et al.*, Nucl. Instrum. Methods A **288**, 389 (1990).

[32] B. von Przewoski *et al.*, Phys. Rev. E **68**, 046501 (2003).

[33] See T.M. Ito *et al.*, Phys. Rev. Lett. **92**, 102003 (2004) and references therein; also K.A. Anoil *et al.*, Phys. Rev. Lett. **82**, 1096 (1999).

[34] I.B. Vasserman *et al.*, Phys. Lett. B **198**, 302 (1987).

[35] A.P. Lysenko, A.A. Polunin, and Yu.M. Shatunov, Particle Accelerators **18**, 215 (1986).

[36] OPERA, Electromagnetic Fields Analysis Program, Vector Fields Ltd., 24 Bankside, Oxford OX5 1JE, England.

[37] T. Roser, private communication.

[38] http : //www.ligo.caltech.edu/

[39] A.M. De Riva, *et al.*, Rev Sci. Instrum. **67**, 2680 (1996) "Very high Q frequency-locked Fabry-Perot cavity". The actual length of the Fabry-Perot resonator used in the PVLAS experiment is 6.4m long, while the length of a test resonator they used was 1.7m long.

[40] G. Cantatore, private communication.

[41] E. Commins, private communication.

[42] G.G. Ohlsen and P.W. Keaton, Jr., Nucl. Instrum. Methods **109**, 41 (1973).

[43] V.G. Baryshevski, LANL/Cornell archive hep-ph/0109099; hep-ph/0201202.

[44] I. Meshkov, Proceedings of EPAC 2004, Lucerne, Switzerland.